Innovative strategies, methods and tools for occupational risks management of manufactured nanomaterials (MNMs) in the construction industry

EXPERIMENTAL ASSESSMENT OF THE EFFICIENCY OF CURRENT PERSONAL DERMAL PROTECTION EQUIPMENT USED IN THE CONSTRUCTION SECTOR

Scaffold Public Documents - Ref.: Scaffold SPD25

Delphine Boutry, Jean-François Damlencourt (CEA)

31/06/2014

The Scaffold research has received funding from the European Community's Seventh Framework Programme (FP7/20072013) under grant agreement number 280535.

INDEX

1. EXECUTIVE SUMMARY

This report concerns the characterization of Personal dermal Protection Equipment's (PPE) efficiency toward the nano exposition via solid phase (nanopowder), aerosol phase (nanoaerosol) and liquid phase (nanohydrosol). Gloves, masks and tyveks used in real scenarios in the construction sector were sent by industrial partners. The purpose of this study was to detect if nanopowders can diffuse through these PPEs. Industrial partners gave also nanopowders and suspensions containing NPs which were added in the different mortars for diffusion experiments. The second part of the study is based on the efficiency of the selected clothes towards NPs diffusion, whether aerosol diffusion and liquid diffusion. Three types of clothes that have been chosen due to their comfortableness to the cold and heat and due to their ability to resist to strong efforts and to evacuate the transpiration. The aim of these studies is to evaluate the efficiency of PPEs and worker clothes in order to give conclusions on the composition of the different clothes to guide industrials in their choice of clothes.

All the PPEs involved in real scenarios (gloves, masks, tyveks) showed that they were enough efficient in standard conditions, i.e. when NPs were in low concentration in mortar (not accidental case). Concerning the clothes used by workers in the construction sector, the rain coating composed of polyamide and polyurethane was the most efficient, whether aerosol diffusion or liquid diffusion. The fact that this material was impermeable prevented the diffusion of NPs. Material that was not woven (fleece jacket) was the most efficient towards aerosolized NPs because it seemed that the NPs were caught inside the material due to its large thickness. But when immersed in a liquid, this material swelled and speed up the diffusion kinetics. The polyester 65%/cotton 35% material was the less efficient towards aerosolized particles but it was more efficient than the fleece jacket when liquid diffusion was operated. Important parameters that reduced NPs diffusion were the thickness of the cloth (the more thick is the cloth, the less NPs diffuse) and the fact that the cloth is woven or non-woven (woven materials cannot swell in liquid).

2. OBJECTIVE

In the first part of this report, we analyse PPEs (gloves, masks, Tyvek) used in 5 real scenarios:

1) Manufacturing of mortar at EUROCEM
2) Applying a mortar in a wall by TOLSA
3) Spraying sol-gel mortar in a wall by TOLSA
4) Demolishing work-cabin at ACCIONA
5) Producing of TiO_2 nanoparticles at TECNAN

In the second part, we characterize the efficiency of 3 types of cloth generally used by workers on construction sites:

1) Fleece jacket composed of 100% of polyester
2) A blend of 65% polyester and 35% cotton (jacket or pants)
3) A double layer rain coating composed of polyamide and polyurethane

The NPs investigated were:

1) Nano SiO_2 given by TECNAN
2) Nano TiO_2 given by TECNAN
3) Nanocellulose given by ACCIONA
4) Nanoclay given by Netcomposites

3. RESULTS

A) SEM-EDX studies of different PPEs used in real scenarios:

Five scenarios have been selected, coming from different stages of the life cycle of NPs:

1) Manufacturing of mortar at EUROCEM
2) Applying a mortar in a wall by TOLSA
3) Spraying sol-gel mortar in a wall by TOLSA
4) Demolishing work-cabin at ACCIONA
5) Producing of TiO_2 nanoparticles at TECNAN

Industrials partners send us all the PPEs that they used during the different scenarios. Three types of gloves have been wearied, one type of mask and one type of Tyvek (Figure 1).

Figure 1: Gloves, mask and tyvek used in real scenarios.

The aim of this study was to observe all the PPEs outside and inside by Scanning Electronic Microscopy (SEM) and to make a chemical analysis on each side in order to detect if NPs contained in the mortar can pass through the PPEs during their use. For all the samples, 3 magnifications have been investigated (X 1000, X 10 000 and X 100 000).

Three different mortars have been investigated. The composition of the mortars are shown in Table 1. Mortar A is a conventional one composed of cement, sand (with silica) and conventional additives. Mortar B is composed of mortar A and additive B containing magnesium, silica and titanium. Mortar C is composed of mortar A and additive C containing nano titanium particles.

Material used			State	Sample ref.
1	Mortar A	Conventional components for 1 ton: 200kg cement + sand (lime, marmoline, SiO_2) + 3,7kg conventional additive	Powder	Mortar A
2	Mortar B	Conventional components and Additive B (0,8%) (Mg, SiO_2, Ti)	Powder	Mortar B
3	Mortar C	Conventional components and Additive C (0,4%) Nano TiO_2	Powder	Mortar C
4	Additive B	Additive B Innoclean DC (sepiolite $Mg_4Si_6O_{15}(OH)_2.6H_2O$ functionalized titania)	Powder	Additive B
5	Additive C	Additive C nano TiO_2 AEROXIDE from Evonix	Powder	Additive C

Table 1: Composition of the third mortars studied.

1) **First scenario: Manufacturing of mortar at Eurocem.**

The tasks involved were:

- Conventional additive and nanomaterial weighting
- Addition of additives to the automatic mixer (the mixer weights and adds the rest of the components automatically)
- Mortar bagging

These tasks were repeated three times, each one with different materials. Figure 2 shows the manufacturing of the mortar and Table 2 summarizes the PPEs used for the manufacturing of the three different mortars.

Figure 2: Different images of the real scenario 1 at EUROCEM.

	Material used	PPE ref.	Sample ref.
0	Reference PPE (without using)	Glove	No available
		Mask	Ref-mask-1
1	Mortar A	Glove	EU-glo-A
		Mask	EU-mask-A
2	Mortar B	Glove	EU-glo-B
		Mask	EU-mask-B
	Mortar C	Glove	EU-glo-C
3		Mask	EU-mask-C

Table 2. Commercial and internal references of the PPEs used for the manufacturing of three types of mortar.

SEM images were done for all the samples outside and inside, see Figures 3, 4 and 5.

EDX measurements were done on all the PPE reference (if provided), on all additives (B and C) and on all mortars (A, B, C). Several elements were found in gloves, mortars and additives as carbon, oxygen, calcium, sulfur and aluminum which could come from the chemical nature of the PPEs but also from the mortar. In order to give the right conclusions concerning the possible diffusion of mortars through the PPEs, we focused our observation on other elements as magnesium, silica and titanium which were only observed in additives and respective mortars.

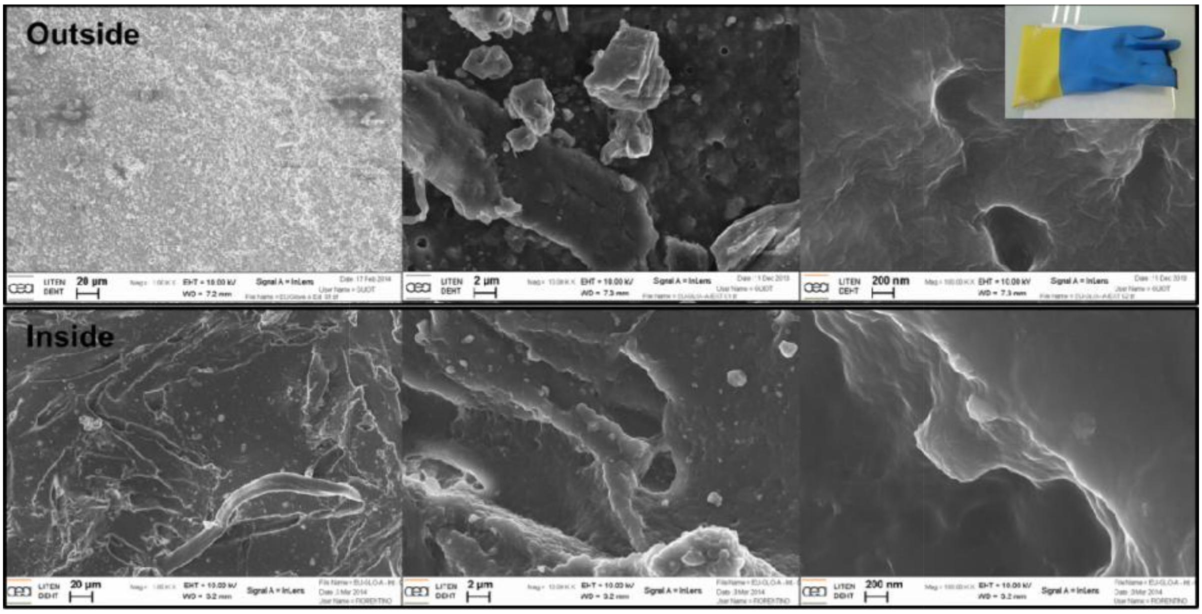

Figure 3: SEM characterization of EU-GLO-A.

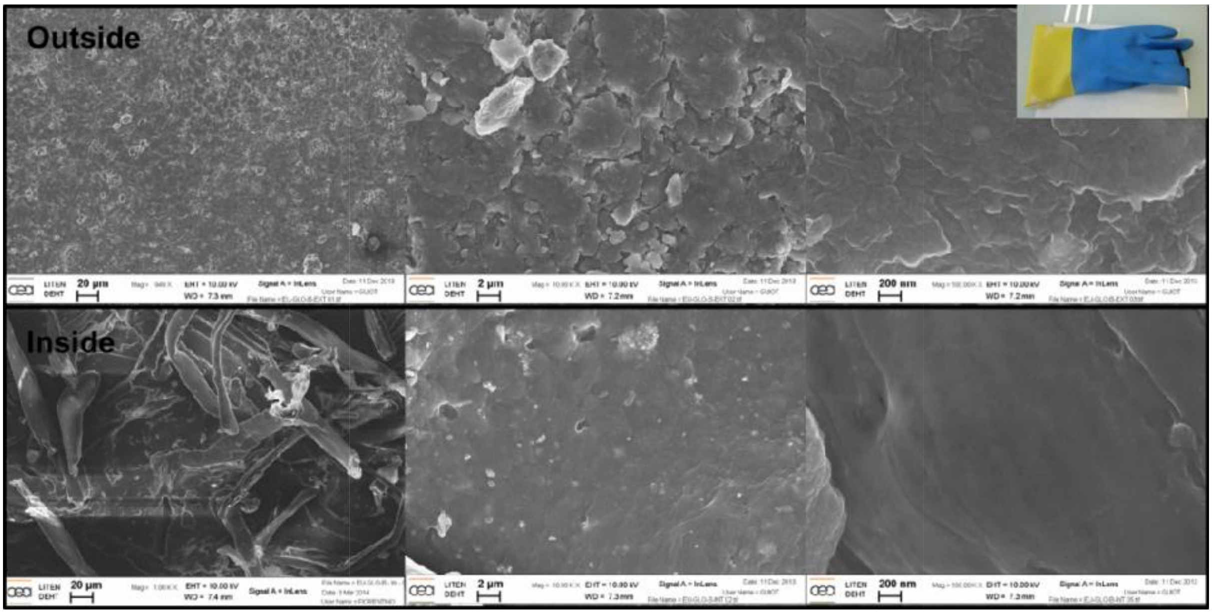

Figure 4: SEM characterization of EU-GLO-B.

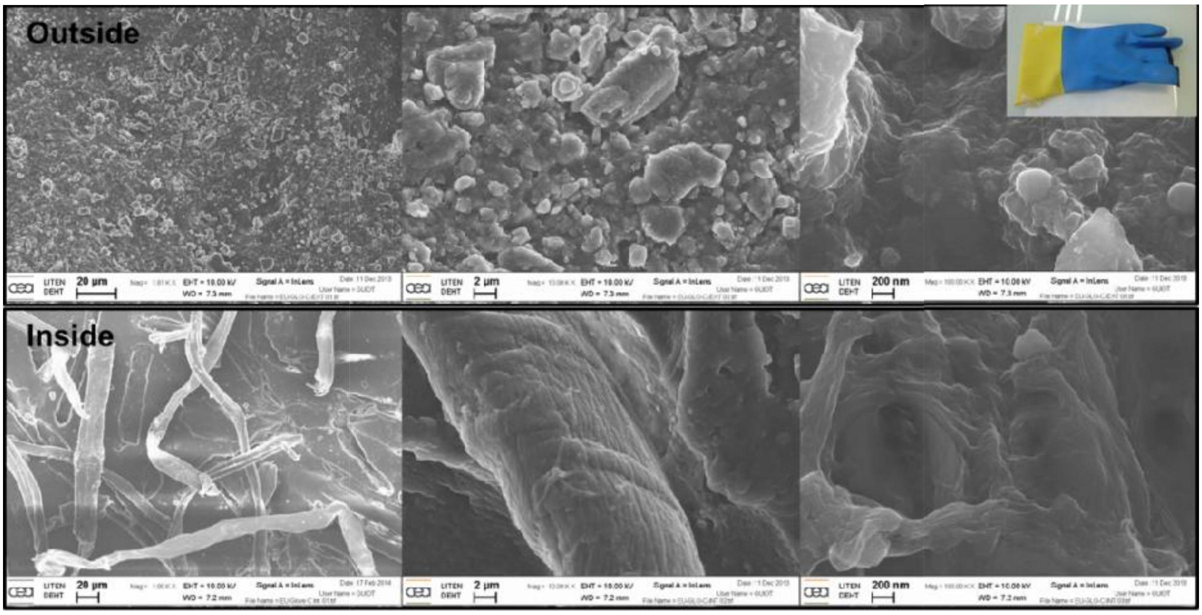

Figure 5: SEM characterization of EU-GLO-C.

Element Energy	C 0,3	O 0,5	Ca 0,3/3,7	S 2,25	Zn/Na 1	Al 1,5	Mg 1,22	Si 1,75	Ti 4,5	Cl 2,6
Ref-glo-1 out. na	-	-	-	-	-		-	-	-	
Ref-glo-1 ins. na	-	-	-	-	-		-	-	-	
Mortar A	✓	✓	✓	✓		✓	✓	✓	-	
EU-glo-A out.	✓	✓	✓	✓	✓	✓	✓	✓	-	✓
EU-glo-A ins.	✓	✓	✓	✓	✓		nd	nd	-	✓
Additive B	✓	✓				✓	✓	✓	✓	
Mortar B	✓	✓	✓	✓		✓	✓	✓	✓	
EU-glo-B out.	✓	✓	✓	✓	✓	✓	✓	✓	✓	✓
EU-glo-B ins.	✓	✓	✓	✓	✓		nd	nd	nd	✓
Additive C	✓	✓					-	-	✓	
Mortar C	✓	✓	✓	✓		✓	✓	✓	✓	
EU-glo-C out.	✓	✓	✓	✓	✓	✓	✓	✓	✓	✓
EU-glo-C ins.	✓	✓	✓	✓	✓		nd	nd	nd	✓

Table 3: EDX measurements on gloves used in scenario 1.

Mortar A had no additives and was composed of cement and sand that contained Magnesium and SiO_2. By analyzing gloves “Eu-glo-A” in an area that contains mortar, magnesium and silica were observed outside of the gloves but were not observed inside the gloves as seen on Table 3.

Mortar B that contained additive B is composed of magnesium, silica and titanium. As for the mortar A, all the elements were detected outside the glove but not inside the glove.

Mortar C is composed of additive C that contained only titanium. Magnesium, silica and titanium were observed in the mortar because magnesium and silica came from the mortar. As for the mortar A and B, all the elements were detected outside the glove but not inside the glove.

Several PPEs were characterized in the same way. The same images were done for each PPE involved in the different scenarios. The other images were included at the end of this document in the appendix.

As for the gloves, masks used in scenario 1 were characterized and no element coming from the mortars were observed inside (see Table 4).

Element Energy	C 0,3	O 0,5	Ca 0,3/3,7	S 2,25	Zn/Na 1	Al 1,5	Mg 1,22	Si 1,75	Ti 4,5	Cl 2,6
Ref-mask-1 out.	✓	✓					-	-	-	
Ref-mask-1 ins.	✓	✓					-	-	-	
Mortar A	✓	✓	✓	✓		✓	✓	✓	-	
EU-mask-A out.	✓	✓	✓				✓	✓	-	
EU-mask-A ins.	✓	✓	✓				nd	nd	-	
Additive B	✓	✓				✓	✓	✓	✓	
Mortar B	✓	✓	✓	✓		✓	✓	✓	✓	
EU-mask-B out.	✓	✓	✓	✓		✓	✓	✓	✓	
EU-mask-B ins.	✓	✓	✓				nd	nd	nd	
Additive C	✓	✓					-	-	✓	
Mortar C	✓	✓	✓	✓		✓	✓	✓	✓	
EU-mask-C out.	✓	✓	✓				✓	✓	✓	
EU-mask-C ins.	✓	✓					nd	nd	nd	

Table 4: EDX measurements on masks used in scenario 1.

2) Second scenario: Applying mortar on a wall.

Tasks involved were:

- Addition of water to the mortar
- Mixing
- Application of the mortar in a wall
- Scraping of the wall (this task was performed after the mortar was completely dry)

The mortar used in TOLSA was the same that was manufactured at EUROCEM the day before. All the mortars were just mixed with water. These tasks were repeated three times. The application of the three materials was made in three different areas of the same wall (see Figure 6).

Figure 6: Different images showing the real scenario 2 at TOLSA.

The PPEs used are collected in Table 5. The different PPEs were used only during the application. In the scraping task, no PPEs were collected because the workers used their own PPEs.

	Material used	PPE ref.	Sample ref.
0	Reference PPE (without using)	Glove	Ref-glo-2
		Mask	Ref-mask-1
1	Mortar A. Application	Glove	T01-glo-A
		Mask	TO1-mask-A
3	Mortar B. Application	Glove	T01-glo-B
		Mask	TO1-mask-B
5	Mortar C. Application	Glove	T01-glo-C
		Mask	TO1-mask-C

Table 5: Commercial and internal references of the PPEs used for the application of the mortar.

Element	C	O	Ca	S	Zn/Na	Al	Mg	Si	Ti
Energy	0,3	0,5	0,3/3,7	2,25	1	1,5	1,22	1,75	4,5
Ref-glo-2 out.	✓	✓	✓	✓	✓		-	-	-
Ref-glo-2 ins.	✓	✓			✓		-	-	-
Mortar A	✓	✓	✓	✓		✓	✓	✓	-
T01-glo-A out.	✓	✓	✓	✓	✓	✓	✓	✓	-
T01-glo-A ins.	✓	✓			✓		nd	nd	-
Additive B	✓	✓				✓	✓	✓	✓
Mortar B	✓	✓	✓	✓		✓	✓	✓	✓
T01-glo-B out.	✓	✓	✓	✓	✓	✓	✓	✓	✓
T01-glo-B ins.	✓	✓			✓		nd	nd	nd
Additive C	✓	✓					-	-	✓
Mortar C	✓	✓	✓	✓		✓	✓	✓	✓
T01-glo-C out.	✓	✓	✓	✓	✓	✓	✓	✓	✓
T01-glo-C ins.	✓	✓			✓		nd	nd	nd

Element	C	O	Ca	S	Al	Mg	Si	Ti
Energy	0,3	0,5	0,3/3,7	2,25	1,5	1,22	1,75	4,5
Ref-mask-1 out.	✓	✓				-	-	-
Ref-mask-1 ins.	✓	✓				-	-	-
Mortar A	✓	✓	✓	✓	✓	✓	✓	-
T01-mask-A out.	✓	✓	✓			✓	✓	-
T01-mask-A ins.	✓	✓				nd	nd	-
Additive B	✓	✓			✓	✓	✓	✓
Mortar B	✓	✓	✓	✓	✓	✓	✓	✓
T01-mask-B out.	✓	✓	✓		✓	✓	✓	✓
T01-mask-B ins.	✓	✓				nd	nd	nd
Additive C	✓	✓				-	-	✓
Mortar C	✓	✓	✓	✓	✓	✓	✓	✓
T01-mask-C out.	✓	✓	✓		✓	✓	✓	✓
T01-mask-C ins.	✓	✓				nd	nd	nd

Table 6: EDX measurements on gloves and masks used in scenario 2.
By regarding EDX measurements on Table 6, the same conclusions can be done for scenario 2. No element coming from the mortars have been detected inside the gloves and the masks.

3) Scenario 3: Applying sol-gel in a wall.

Tasks involved were:

- Spraying in a wall: sol-gel application, spray with 1.3-1.7 % of nanoTiO_2 (see Figure 7).

This task was repeated twice, each one with different materials as it is shown in the next table 7.

Figure 7: Image of the real scenario 3 at TOLSA.

	Material used	State
1	Sol-gel A	Suspension
2	Sol-gel B	Suspension

Table 7: Materials used for the spraying of the wall.

PPEs used to perform the two spray applications are shown in the next table 8.

	Material used	PPE ref.	Sample ref.
0	Reference PPE (without using)	Glove	Ref-glo-2
		Mask	Ref-mask-1
		Tyvek coverall	No available
1	Sol-gel A and B	Glove	T02-glo-AB
		Mask	TO2-mask-AB
		Tyvek coverall	T02-Tyvek-AB

Table 8: Commercial and internal references of the PPEs used for the spraying applying.

Element Energy	C 0,3	O 0,5	Ca 0,3/3,7	S 2,25	Zn/Na 1	Al 1,5	Mg 1,22	Si 1,75	Ti 4,5	Cl 2,6
Ref-glo-2 out.	✓	✓	✓	✓	✓		-	-	-	
Ref-glo-2 ins.	✓	✓					-	-	-	
T02-glo-AB out.	✓	✓	✓	✓	✓	✓	✓	✓	✓	
T02-glo-AB ins.	✓	✓					nd	nd	nd	
Ref-mask-1 out.	✓	✓					-	-	-	
Ref-mask-1 ins.	✓	✓					-	-	-	
T02-mask-AB out.	✓	✓	✓	✓			nd	✓	nd	
T02-mask-AB ins.	✓	✓					nd	nd	nd	
Ref-tyvek out.	na	na	na	na	na	na	na	na	na	na
Ref-tyvek ins.	na	na	na	na	na	na	na	na	na	na
T02-tyvek-AB out.	✓	✓	✓				nd	✓	nd	
T02-tyvek-AB ins.	✓	✓					nd	nd	nd	

Table 9: EDX measurements on PPEs used in scenario 3.

We saw that also in this case, no element passed through the PPEs whether gloves, masks or tyveks (see Table 9). As we knew, sol-gel A and B contained nano titanium particles but we only detected titanium on the outside part of the gloves and not outside of masks and tyveks. We thought that when spraying on a wall, only PPEs that were closed to the spray gun can be in contact with all the components of the suspension. That's why we found titanium outside the gloves and not outside masks and tyveks. It seemed that nanoTiO_2 was less volatile than the other components of the sol gel solution. Nevertheless, no titanium was detected inside the gloves.

4) Scenario 4: Demolishing work cabin at ACCIONA

Tasks involved were:

- Demolition of the cabin
- Waste collection

These tasks were performed for each work-cabin and each cabin was covered with the materials listed below in Table 10.

	Material used		State
1	Cabin A	The walls of the cabin were covered with a layer of mortar containing 2% of nanoSiO_2	Solid
2	Cabin B	The walls of the cabin were covered with a layer of mortar containing 2% of TiO_2	Solid

Table 10: Materials used for the covering of the work-cabins.

Only one mask was used in Acciona during the demolition of the Cabin B (see table 11).

	Material used	PPE ref.	Sample ref.
1	Cabin A	*No PPE was used*	
2	Cabin B	Mask	AC-mask-B

Table 11. Commercial and internal references of the PPEs used for the demolition.

During the demolition of the cabin, no element of the mortar B were observed inside the masks whereas they were detected outside (Table 12).

Element Energy	C 0,3	O 0,5	Ca 0,3/3,7	S 2,25	Al 1,5	Mg 1,22	Si 1,75	Ti 4,5
Additive B	✓	✓			✓	✓	✓	✓
Mortar B	✓	✓	✓	✓	✓	✓	✓	✓
AC-mask-B out.	✓	✓	✓	✓	✓	✓	✓	✓
AC-mask-B ins.	✓	✓				Not detected	Not detected	Not detected

Table 12: EDX characterization of PPEs used in scenario 4.

5) Scenario 5: Producing nanoTiO2 at TECNAN

TiO_2 was produced at Tecnan. Tasks involved were:

- Reaction (no PPE were used)
- Collection of TiO_2

- Transferring of TiO_2 to little containers
- Cleaning of filters
- The material produced in this process was nanoTiO_2 in powder state. See Figure 8.

PPEs used:

- Gloves:
    - o two pair of gloves during collection & transferring [nitrile blue a) below nitrile green b) simultaneously]
    - o two pair of gloves (new) during cleaning [nitrile blue a) below nitrile green b) simultaneously]
- Tyvek coverall:
    - o The same Tyvek coverall during collection+ transferring + cleaning.

All these PPEs are listed in Table 13.

	Material used	**PPE ref.**	**Sample ref.**
0	Reference PPE (without using)	Glove	No available
		Glove	No available
		Tyvek coverall	No available
1	Collection and Transferring	Glove a)	TEC11-glo
		Glove b)	TEC12-glo
2	Cleaning	Glove a)	TEC21-glo
		Glove b)	TEC22-glo
		Tyvek coverall	TEC23-tyvek

Table 13: Commercial and internal references of the PPEs used for the TiO_2 production.

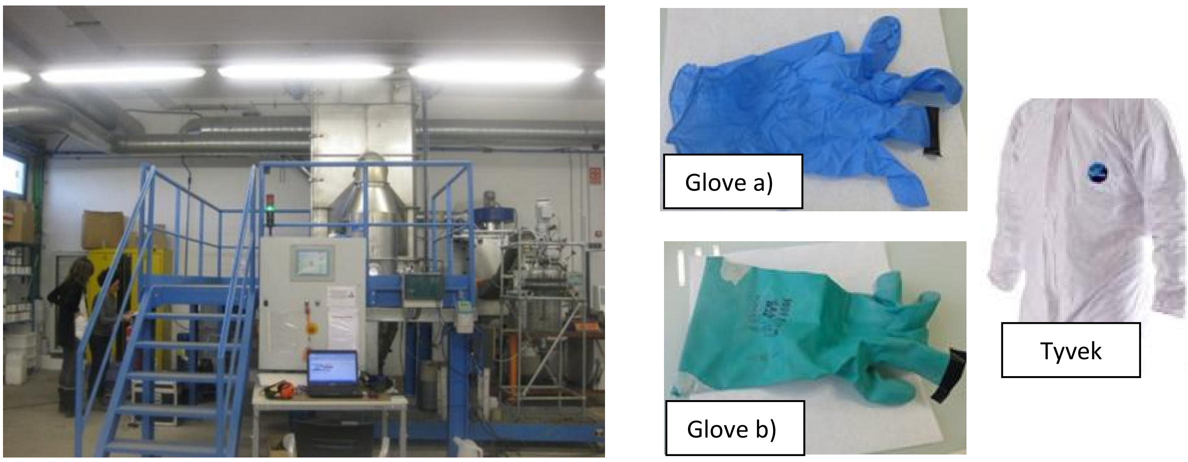

Figure 8: Image of the real scenario 5 at TECNAN and PPEs used during this stage.

Element Energy	C 0,3	O 0,5	Ca 0,3/3,7	S 2,25	Zn/Na 1	Al 1,5	Mg 1,22	Si 1,75	Ti 4,5	Cl 2,6
Ref-glo-11/21 out.	na	na	na	na	na	na	na	na	na	na
Ref-glo-11/21 ins.	na	na	na	na	na	na	na	na	na	na
TEC11-glo out.	✓	✓	✓	✓	✓		-	nd	✓	
TEC11-glo ins.	✓	✓	✓	✓	✓		-	nd	nd	
TEC21-glo out.	✓	✓	✓	✓	✓		-	✓	✓	
TEC21-glo ins.	✓	✓	✓	✓	✓		-	nd	nd	
TEC12-glo out.	✓	✓	✓	✓	✓		-	✓	✓	
TEC12-glo ins.	✓	✓	✓	✓	✓		-	nd	nd	
TEC22-glo out.	✓	✓	✓	✓	✓		-	✓	✓	
TEC22-glo ins.	✓	✓	✓	✓	✓		-	nd	nd	
Ref-tyvek-23 out.	na	na	na	na	na	na	na	na	na	na
Ref-tyvek-23 ins.	na	na	na	na	na	na	na	na	na	na
TEC23-tyvek out.	✓	✓	✓		✓		✓	✓	✓	
TEC23-tyvek ins.	✓	✓	✓		✓	✓	✓	nd	nd	

Table 14: EDX measurements on PPEs used in scenario 5.

Both gloves TEC12 and TEC22 (gloves b) contained silica and titanium outside because they were in direct contact with the titanium. According to Table 14, we observed that these elements were not present inside these gloves while we observed titanium and titanium with silica outside gloves TEC11 and TEC21 (gloves a) below gloves b)) respectively. It seems that during the process, the Ti powder can be inserted between the both gloves a) and b) or there could be a titanium contamination when removing the first gloves b). Nevertheless, no Ti element was found inside the gloves a).

B) Diffusion measurements of nanoparticles through clothes used in the construction sector:

The purpose of this study is to test the diffusion of nanoparticles through different clothes that were used by workers in the construction sector. Three different types of clothes have been selected for this study and they are listed in Table 15 and are showed in Figures 9, 10 and 11.

Type of	Chemical	Density	Thickness	Porosity	Type of PPE

materials	Nature				
Non-woven materials	Polyester 100%	300 - 340 g/m^2	3.8 mm	90-95%	Jacket ; polar
Woven materials	Polyester 65% / cotton 35%	245 - 350 g/m^2	500 microns	50-60%	T-shirt ; jacket
Coated materials	PU coated polyamide	n.a.	340 microns	20-30%	Rain jacket

Table 15: Dermal personal protection equipment's (PPE) selected.

Figure 9: Image of the non-woven material selected, a fleece jacket 100% polyester and two SEM images of this cloth.

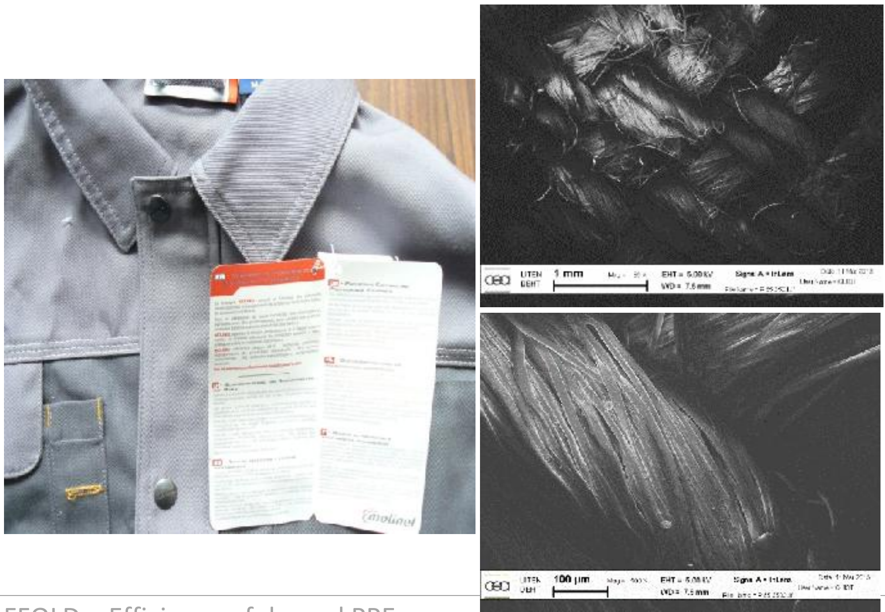

Figure 10: Image of the woven material selected, a polyester 65%/cotton 35% jacket and two SEM images of this cloth.

Figure 11: Image of the coated material selected, a rain jacket polyurethane coated polyamide and two SEM images of this cloth.

1) Aerosol diffusion:

The aerosol diffusion cell is composed of 2 parts separated by a medium. The first part is called “upstream” and the second part is called “downstream”. The image and the diagram of the apparatus are shown in Figure 12.

A generation of nanoaerosol was first done. A liquid suspension containing nanoparticles was aerosolized with a TSI atomizer. The nanoparticles were counted with a CPC (Condensation Particle Counter) and a granulometry is done with a FMPS (Fast Mobility Particles Sizer). The dried aerosol went in the diffusion cell by the upstream side with a controlled rate of flow (1mL/min), diffused through the media (or not) and arrived in the downstream side where nanoparticles were also counted and a granulometry was also done. During the diffusion process, nanoparticles concentration in upper cell was maintained constant (controlled by CPC) and the differential pressure between the both sides was maintained at zero. These tests are derivated from “Through-diffusion” method NF EN 374 and NF EN ISO 6529.

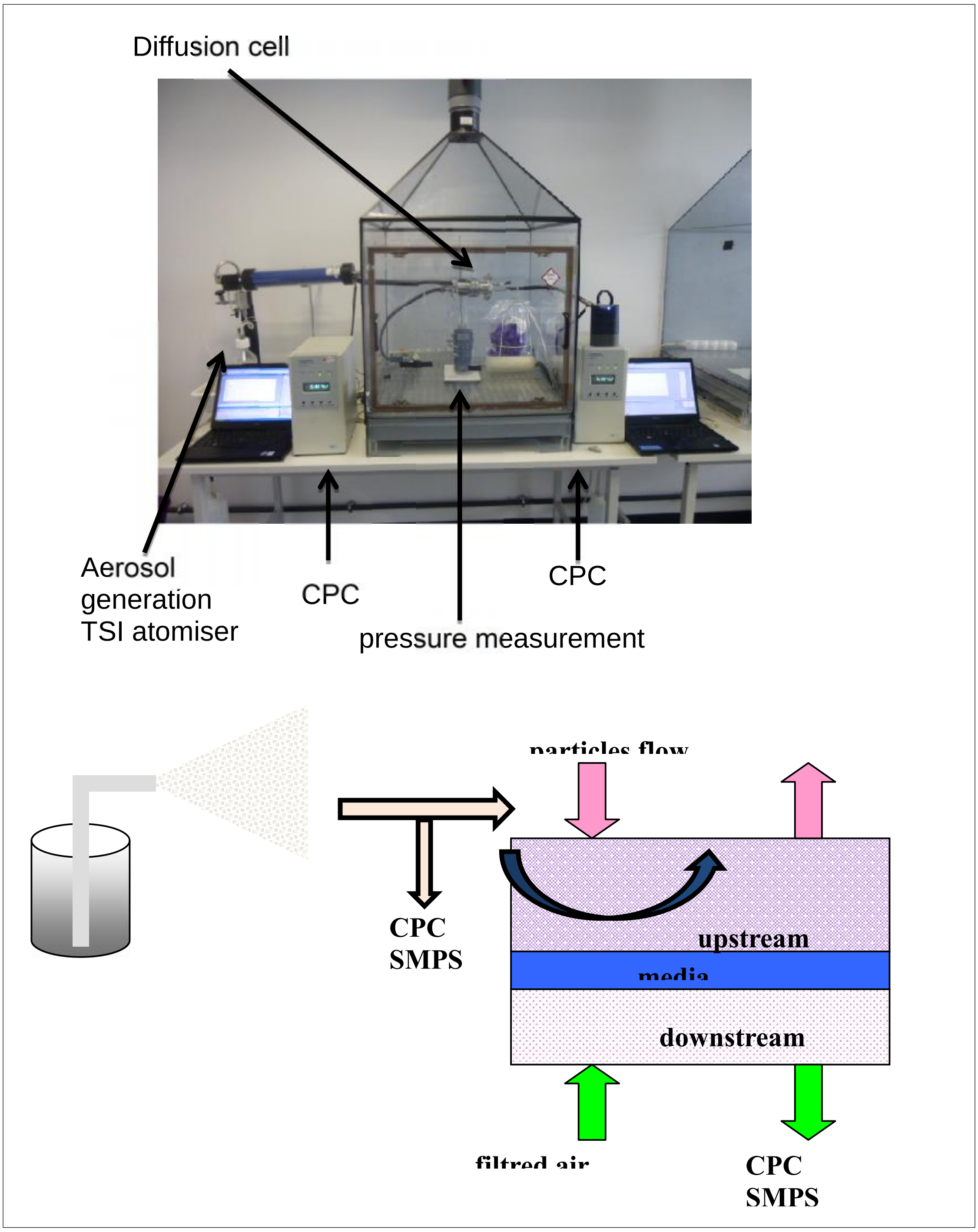

Figure 12: Image of the diffusion cell and drawing of the apparatus.

Different types of nanoparticles have been sent by industrial partners. At first, each NPs were characterized by SEM and/or by TEM in order to know their real size (Figure 13).

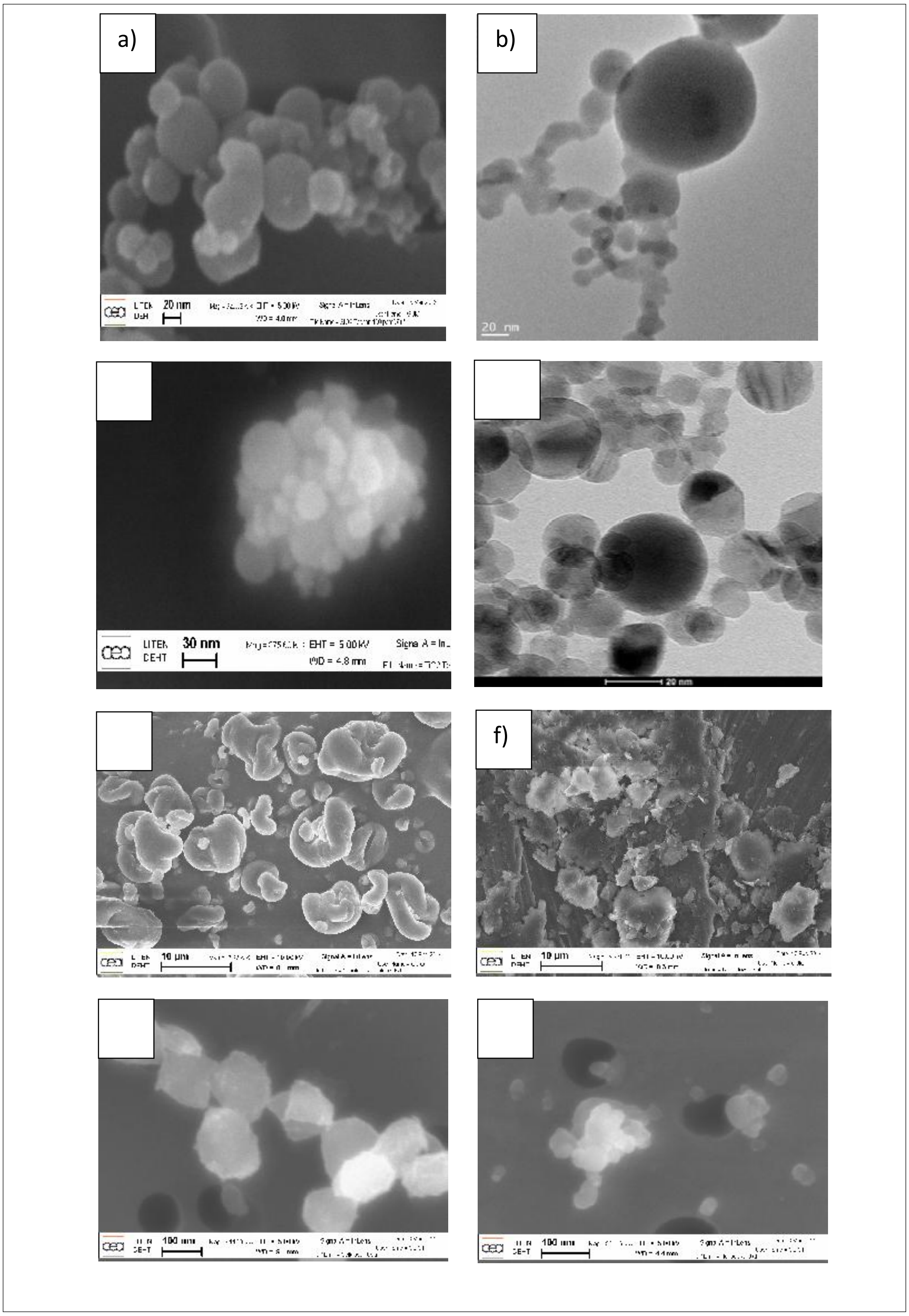

Figure 13: SEM and TEM images of the 4 different types of NPs sent by the industrial partners. a) SEM image of SiO_2 NPs, b) TEM image of SiO_2 NPs, c) SEM image of TiO_2 NPs, d) TEM image of TiO_2 NPs, e) SEM image of nanocellulose, f) SEM image of nanoclay, g) SEM image of aerosolized nanocellulose, h) SEM image of aerosolized nanoclay.

The particle size of SiO_2 and TiO_2 were in the nanometric range (see Figure 13 a), b), c) and d)) but were agglomerated and the average size of the agglomerates measured by DLS was of about 174 nm for SiO_2 in suspension, of about 198 nm for SiO_2 powder, of about 301 nm for TiO_2 in suspension and of about 197 nm for TiO_2 powder (see Table 16). The size of the nanocellulose and the nanoclay were rather in the micrometric range (Figure 13 e) and f)) but when these both powders were put in solution in water and they were aerosolized and collected on filters, their sizes were surprisingly totally different, they reached nanometric ranges.

Size	10ppm	10ppm	100ppm	100ppm
	TiO2 suspension	TiO2 powder (in water)	SiO2 suspension	SiO2 powder (in water)
Size (meas.1)	291.4	228.5	171.3	195.1
Size (meas.2)	308	180.3	175.4	201.1
Size (meas.3)	304.8	180.6	175.7	195.7
Average Size	**301.4**	**196.5**	**174**	**197.3**
RSD %	**2.92**	**14.12**	**1.41**	**1.67**

Table 16: Size of SiO_2 and TiO_2 particles in suspensions and in powders measured by Dynamic Light Scattering (DLS).

All these powders were put in solution and the concentrations were selected in order to have a mean diameter of the aerosolized particles of about 100nm. The generation of aerosols in the nanosize range was obtained by decreasing the concentration of NP in solutions. So that SiO_2 and TiO_2 solutions had concentrations of about 500ppm and nanocellulose and nanoclay solutions had concentrations of about 1000ppm.

By counting the number of particles/cm^3 in the upstream side and in the downstream side of the diffusion cell with CPC, we determined the efficiency of clothes to the different type of NPs (Figure 14 and Table 17).

The first conclusion was that the rain cloth made of a double layer material composed of polyamide and polyurethane was the most efficient to NPs diffusion. No NPs diffused through this cloth, which was not the case for the two other types of cloth. Indeed, the fleece jacket and the 65% polyester/35% cotton material were permeable and let diffuse all the type of nanoparticles. In general, the 65% polyester/ 35% cotton material was the less efficient cloth toward diffusion of aerosolized NPs. This material was very thin and this could explain the fact that all the NPs could diffuse easily through it. Concerning the fleece jacket, its important thickness (3.8mm) must play a retention role, the NPs diffused in the material but a great part must be caught inside the material. We also observed that nano-SiO_2 and nano-TiO_2 particles diffused less than nanocellulose and nanoclay because their percentage in the downstream part were lower. We saw that particles could diffuse through some clothes and we determined the size of these particles to see if all the sizes can diffuse, see Figure 15. A FMPS was connected at the downstream part of the cell and we saw that no SiO_2 NPs (<100nm) observed in the upstream part diffused through all the types of clothes. All the types of cloth are very efficient toward the diffusion of SiO_2 NPs. Concerning TiO_2, NPs diffused only through one type of cloth; the polyester 65%/ cotton 35% material but the diffusion percentage was very low. Nanocellulose and nanoclay had a very different behavior. All the particle sizes detected in the upstream part diffused through the fleece jacket and the 65% polyester/ 35% cotton material and were collected in the downstream part but in smaller proportion. Moreover, the 65% polyester/ 35% cotton material was more permeable than the fleece jacket made of 100% polyester. This can be explained by the thin thickness of the 65% polyester/ 35% cotton material compared to the thickness of the fleece jacket.

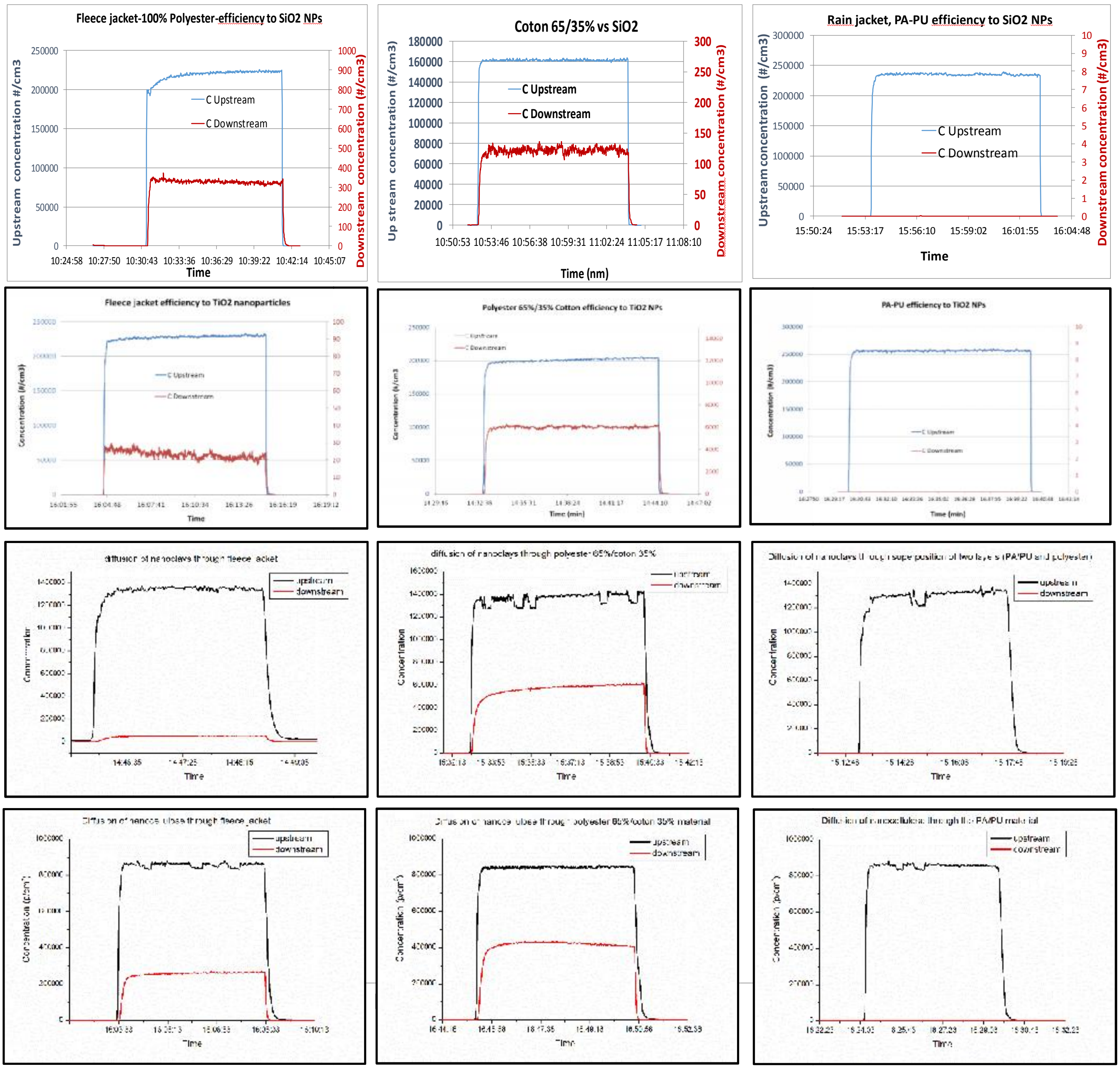

Figure 14: Efficiency of different types of cloth in function of the type of aerosolized NPs.

Materials	nanoTiO2 aerosol	nanoSiO2 aerosol	nanoclay aerosol	nanocellulose aerosol
100% polyester (fleece jacket)	0,01%	0,08%	4%	31%
Polyester 65% / Coton 35%	2,9%	0,14%	43%	50%
PA/PU and Polyester	0%	0%	0%	0%

Table 17: Percentage of different type NPs detected in the downstream part of the diffusion cell.

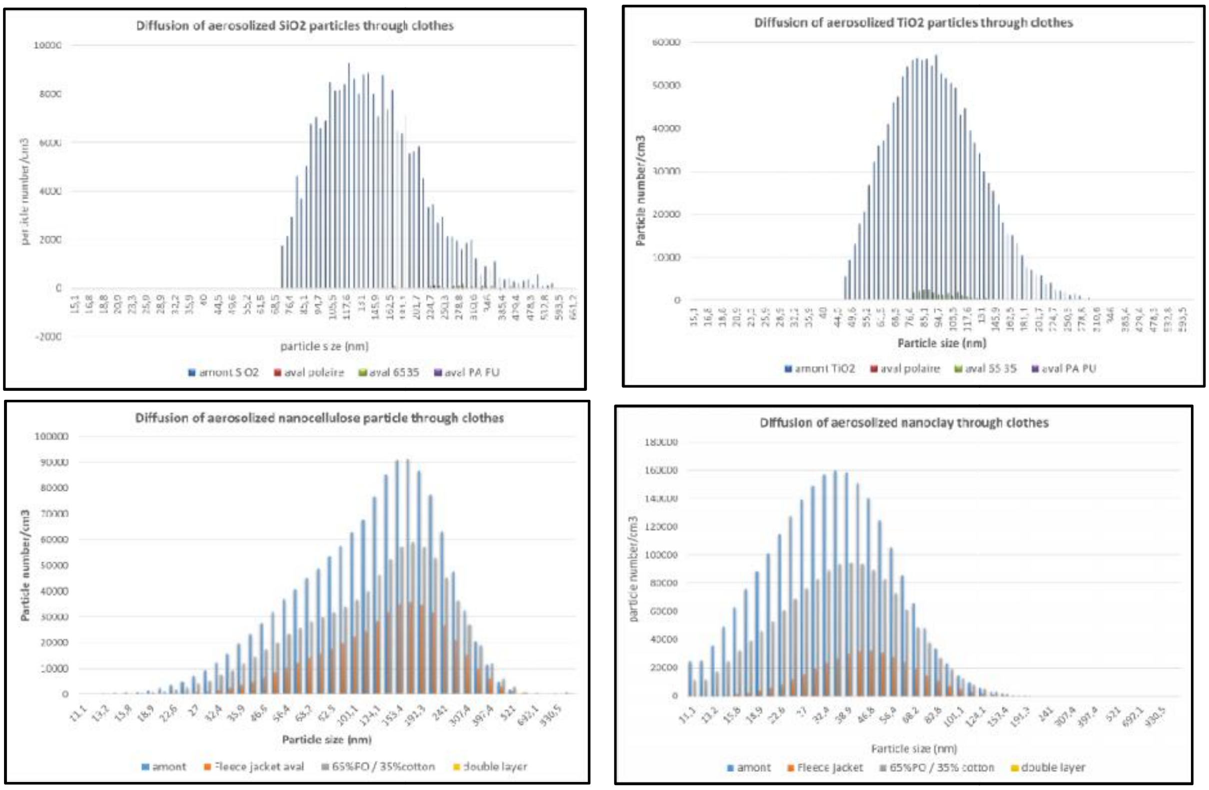

Figure 15: Granulometries obtained in the both parts of the diffusion cell (upstream and downstream) for the different types of NPs and through different cloths.

2) Liquid diffusion:

This phenomenon consists in a displacement of components from high concentration to areas of low concentration. From a phenomenological and first-order point of view, this phenomenon is governed by the Fick law (see Figure 16) where “De” is the diffusion coefficient that we tried to simulate for each cases. The liquid diffusion cell is composed of 2 parts separated by a medium. The first part is called “upstream” and the second part is called “downstream”. The image and the diagram of the apparatus is shown in Figure 16.

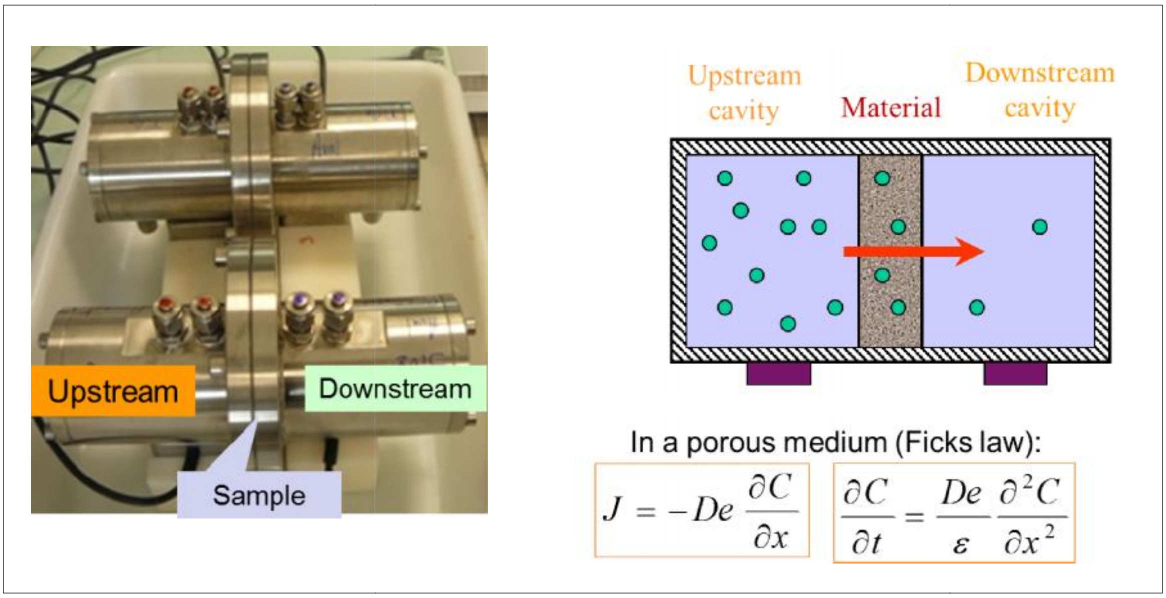

Figure 16: Image and diagram of the liquid diffusion cell used for the experiments and Fick law for one dimension “x”. “J” is the current density vector of particles, “De” is the diffusion coefficient of the particles in a medium and “C” is the concentration of the solution.

The diffusion of SiO_2 nanoparticles through the three types of selected clothes was followed. At first, to test the sealing of the system, diffusion coefficient of NaCl was measured. A solution with a 1M concentration of NaCl in ultrapure water was made (called mother solution). To calculate the species concentration of the NaCl solutions, we measured the conductivity of each samples. The conductivity measurement apparatus was calibrated with 5 different dilutions of the mother solution with ultrapure water: 2.10^{-2} M, 10^{-2} M, 5.10^{-3} M, 10^{-3} M and 10^{-4} M. The calibration curve of the conductivity cell is shown on Figure 17.

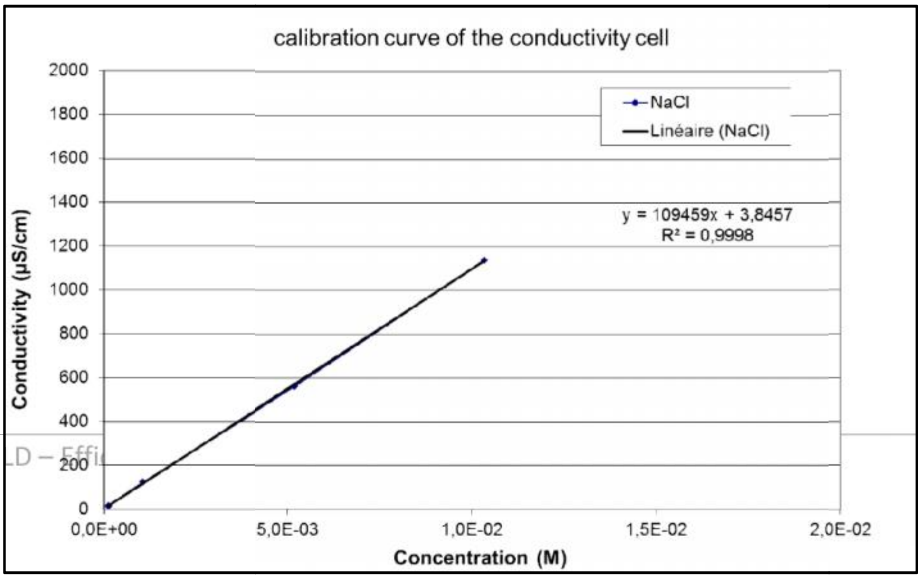

Figure 17: Calibration curve of the conductivity cell.

Three diffusion cells were prepared with three different types of cloth:

1) Cloth = fleece jacket 100% polyester
2) Cloth = 65% polyester and 35% cotton material
3) Cloth = polyamide and polyurethane material

The upstream and downstream parts were filled with ultrapure water, we took 1mL of water in each part to prevent the overflow when we took liquid samples. Then, we took 2mL of water in each part and we put 2 mL of 1M solution of NaCl in the upstream part and 2mL of ultrapure water in the same time in the downstream part to equilibrate the volumes. This manipulation was the beginning of the diffusion kinetic (T0). We took 1mL of solution in the both parts (upstream and downstream) at the same time every half hour at first and every hour for the remainder of the kinetic in the case of one day experiment (fleece jacket). Concerning the diffusion kinetic for the polyester 65% / cotton 35% material, the experiment was made in 2 days and for the PA/PU material, the experiment lasted 11 days. From these three experiments, we obtained the diffusion coefficient of NaCl through the different clothes by fitting experimental datas. To do this, we had to know the thickness and the porosity of the clothes, the surface of the exposed area and the volume of the both upstream and downstream cavities. On Figure 18, 19 and 20, we observe the NaCl normalized concentration in function of time and Table 17 summarizes all the diffusion coefficients measured. For the SiO_2 particles diffusion, the normalized concentration was obtained by Inductively Coupled Plasma Mass Spectrometry (ICPMS). A calibration curve was also done using 7 different dilutions of ionic Si in NaOH solution at pH 11 (10, 20, 50, 100, 150, 200 and 1000 ppb), see Figure 21. Due to ICPMS quantification of Si element, we calculated the Si concentration for all the samples and we plotted the Si normalized concentration in function of time and we also made a simulation of the Si diffusion coefficient through the third clothes when it was possible (see Table 18).

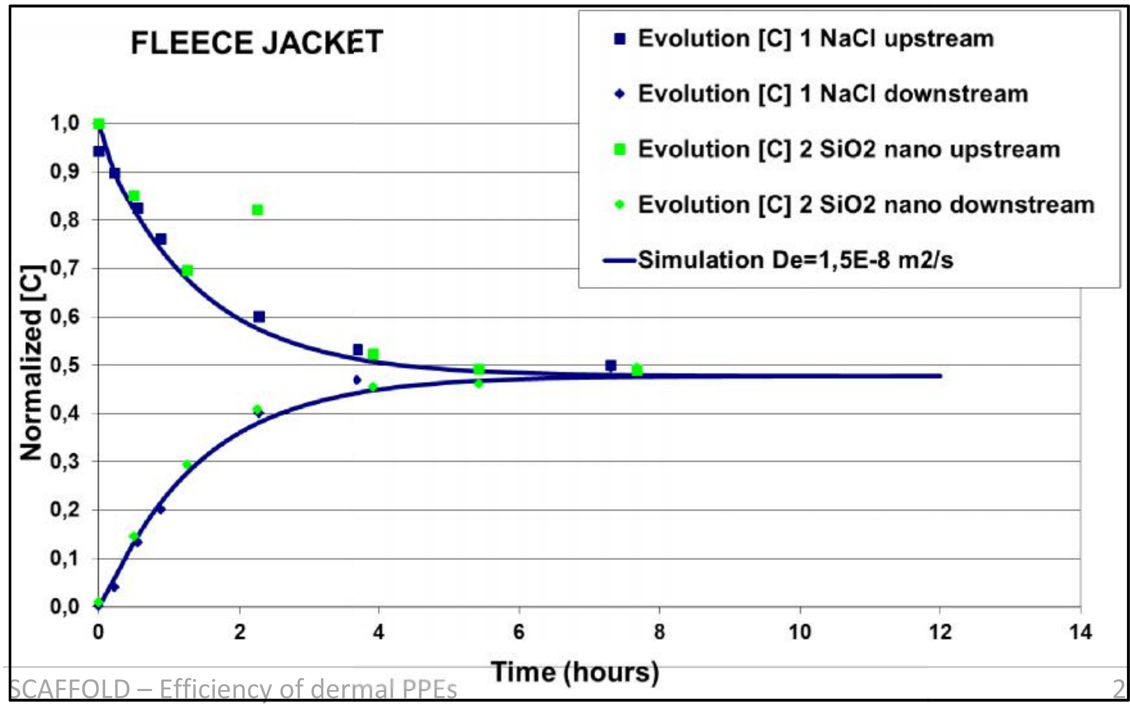

Figure 18: NaCl and SiO_2 diffusion through the fleece jacket 100% polyester. NaCl and SiO_2 normalized concentration in function of time and diffusion coefficient simulation of NaCl and SiO_2 nanoparticles through the fleece jacket.

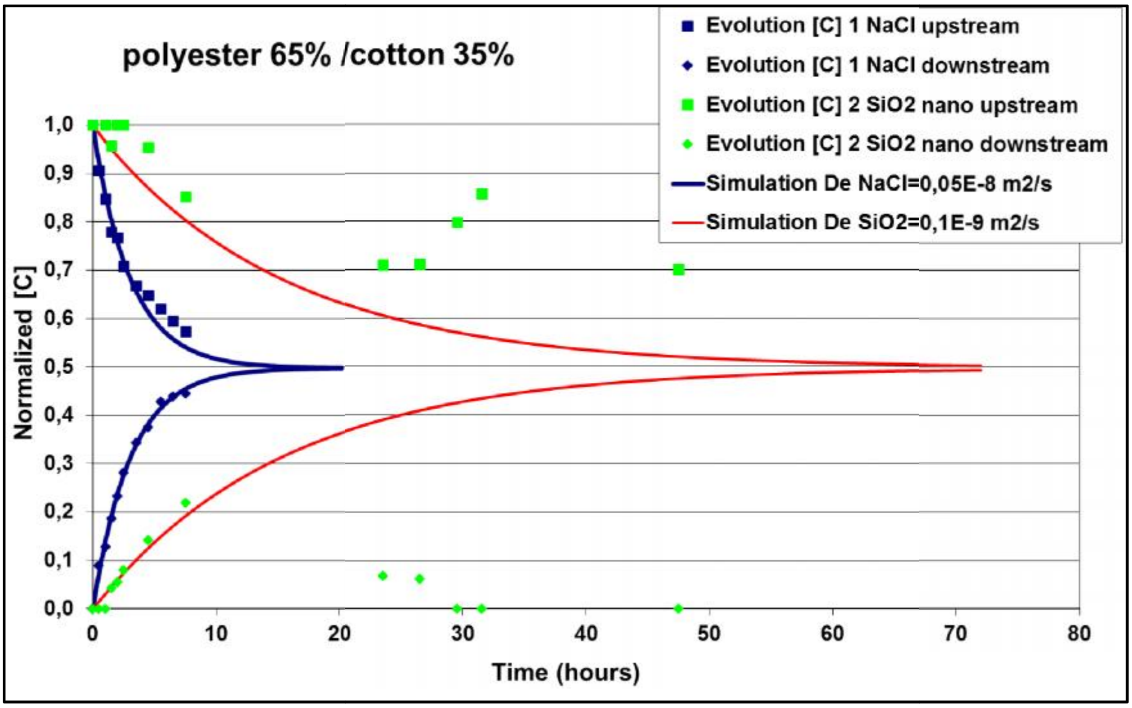

Figure 19: NaCl and SiO_2 diffusion through the 65% polyester/ 35% cotton material. NaCl and SiO_2 normalized concentration in function of time and diffusion coefficient simulation of NaCl and SiO_2 nanoparticles through the 65% polyester/ 35% cotton material.

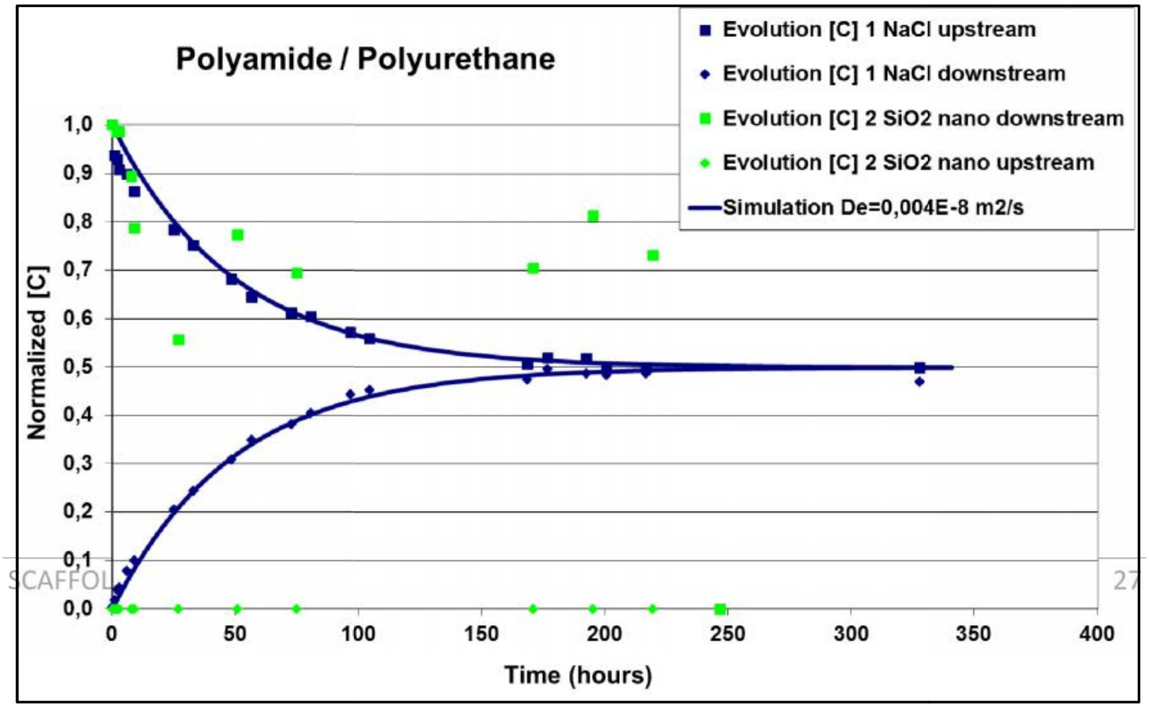

Figure 20: NaCl and SiO_2 diffusion through the polyamide/polyurethane material. NaCl and SiO_2 normalized concentration in function of time and diffusion coefficient simulation of NaCl through the polyamide/polyurethane material.

Material	Diffusion coefficient of NaCl	Diffusion coefficient of SiO_2
Fleece jacket 100% polyester	$1{,}500.10^{-8}$ m^2/s	$1{,}500.10^{-8}$ m^2/s
Polyester 65% / Cotton 35%	$0{,}050.10^{-8}$ m^2/s	$0{,}010.10^{-8}$ m^2/s
Polyamide / Polyurethane	$0{,}004.10^{-8}$ m^2/s	/

Table 18: Diffusion coefficient of NaCl and SiO_2 through different types of cloth.

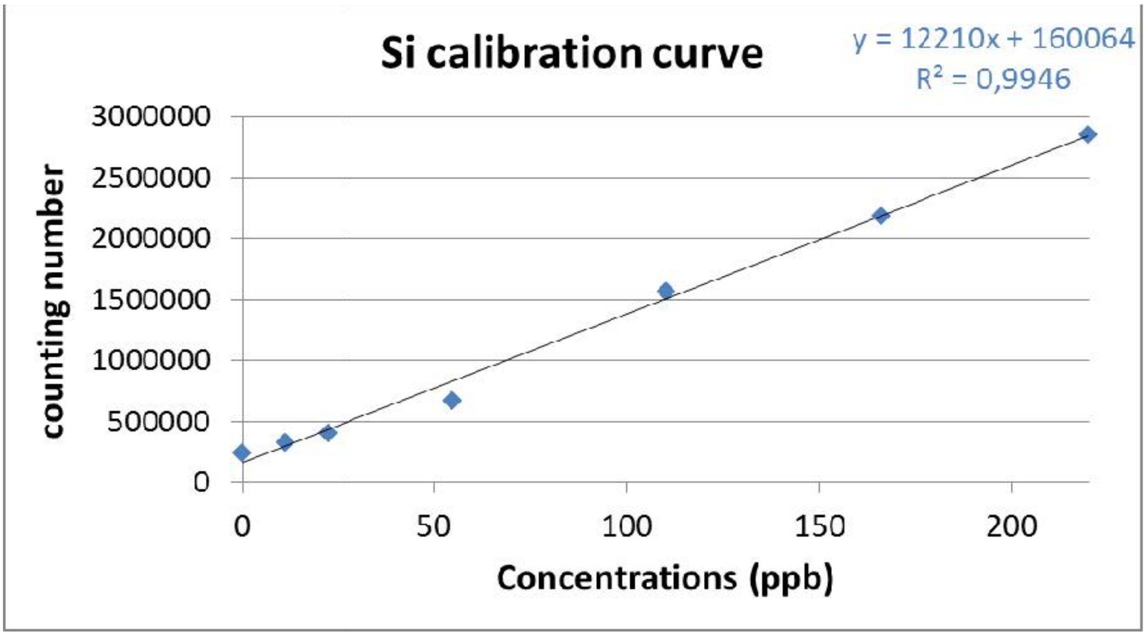

Figure 21: Calibration curve of ionic silica for ICPMS measurements.

We observed that the diffusion coefficients of NaCl and SiO_2 through the fleece jacket were the same and that they were higher than all the other coefficients. For all the other kinetics, a concentration equilibrium between the both parts of the diffusion cell was obtained only with NaCl. It seemed that SiO_2 particles anchored on the cell walls or stayed on/in the clothes. The diffusion of NaCl and SiO_2 through the 65% polyester/35% cotton material had not the same kinetic. The equilibrium with NaCl species was reached in about 15 hours and we observed that SiO_2 particles diffused more slowly than NaCl. Concerning the last cloth, which is a raining cloth composed of two layers of polyamide and polyurethane, only NaCl can diffuse through it but very slowly, the equilibrium between the both parts (upstream and downstream) was obtained in about 200 hours. Even no SiO_2 particles diffused to the downstream part, we observe a decreasing concentration in the upstream part. We though also to a fixing of the particles on the wall of the cell or at the top the cloth. What is very surprising is the fact that the concentration can vary as much between the different samples of a same kinetic. Regarding the ICPMS results, we saw that the Si concentrations were not homogeneous during the kinetics. We observed that concentrations were higher in the upstream part at t=5 and t=11 and in the downstream part at t=7 and t=8 (see Figure 22). We thought that all the samples were not homogeneous and that maybe very big particles could be present in some samples and not in others. Therefore, the size of the particles have been investigated. We made Field Flow Fractionation (FFF) measurements (Figure 23) and Transmission Electronic Microscopy (TEM) observations (Figure 24). We observed with FFF that the rms radii of the particles were in the range between 60 and 700 nm for both upstream and downstream parts and were not single but mainly embedded in a kind of gel. So the size of these clusters were larger than 100nm. We did not see particles whether in FFF or by TEM in downstream of the PAPU experiments, which is in accordance with results obtained in the study of the aerosol diffusion and with the fact that this material is impermeable towards SiO_2.

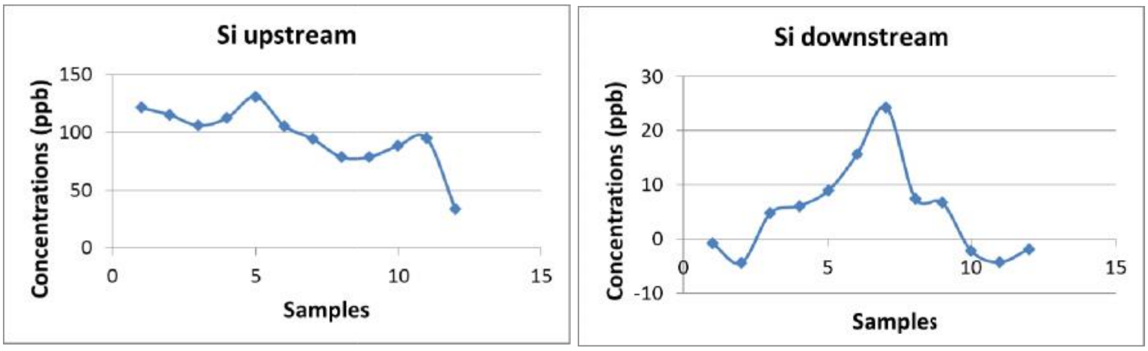

Figure 22: Si concentration in the upstream and downstream parts of the diffusion cell obtained by ICPMS in function of the samples (1 was the first sample, 12 was the last samples).

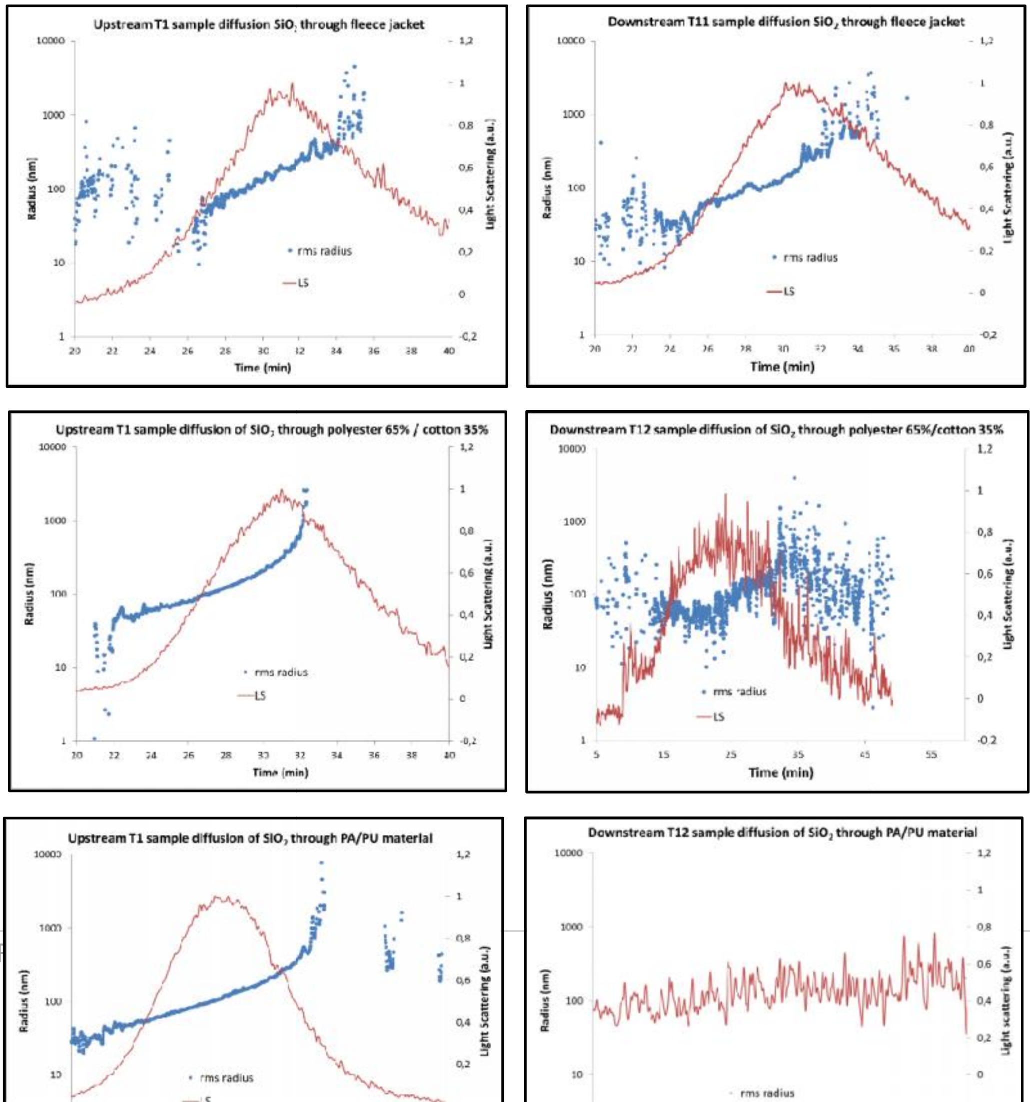

Figure 23: FFF measurements on the first upstream sample and on the last downstream sample of SiO_2 diffusion experiment through fleece jacket, polyester 65% / cotton 35% and PA/PU.

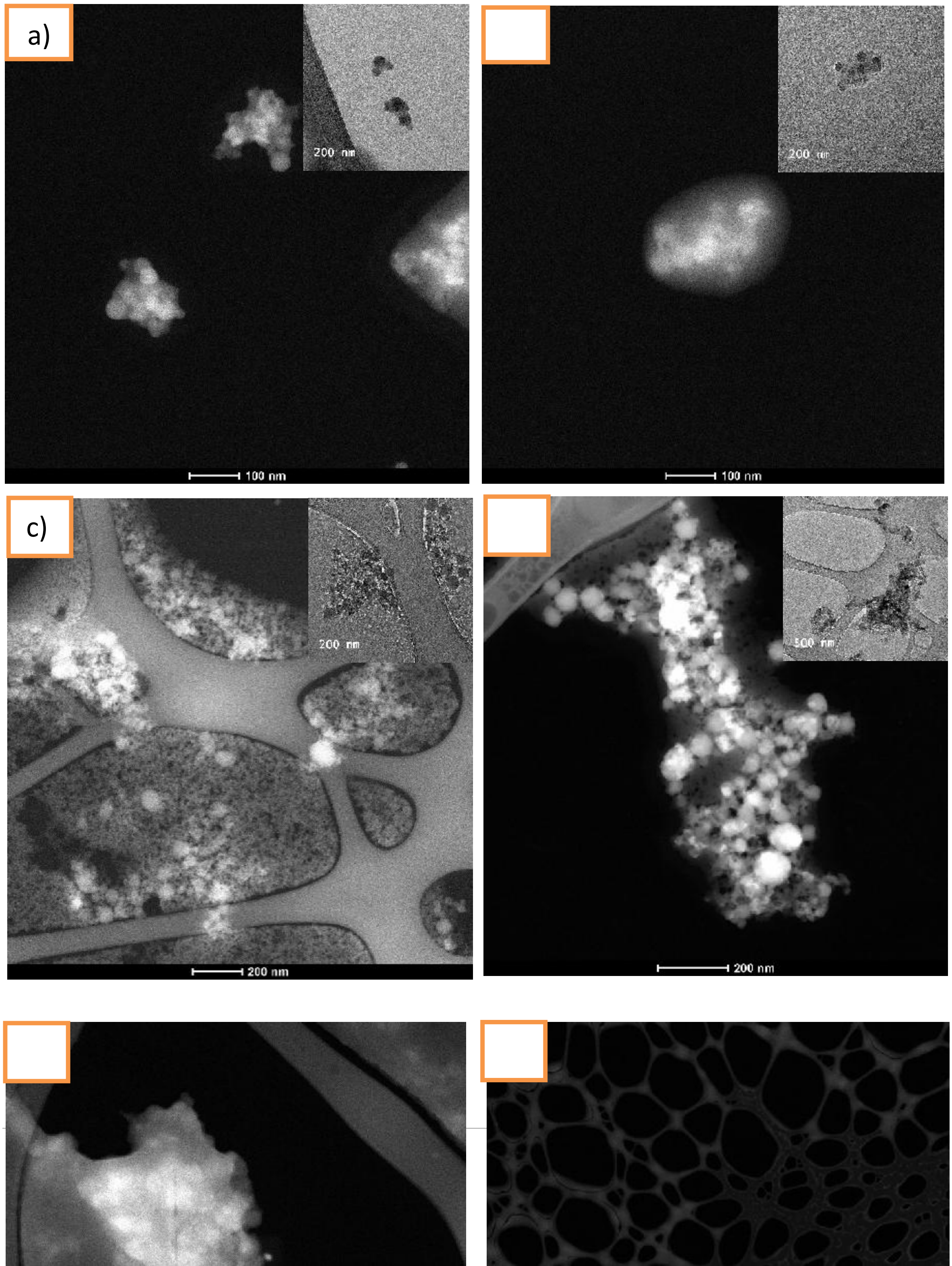

Figure 24: STEM and TEM images of **a)** upstream liquid took at the beginning of the diffusion kinetic through the fleece jacket and **b)** downstream liquid took at the end of the diffusion kinetic through the fleece jacket, **c)** upstream liquid took at the beginning of the diffusion kinetic through the 65% polyester/35% cotton material and **d)** downstream liquid took at the end of the diffusion kinetic through the 65% polyester/35% cotton material, **e)** upstream liquid took at the beginning of the diffusion kinetic through the PAPU material and **f)** downstream liquid took at the end of the diffusion kinetic through the PAPU material.

4. DISCUSSION

Analysis made during this project bring different results. The part focused on the observation of PPEs involved in real scenarios in industrial partners showed that the actual gloves, masks and tyveks are efficient enough towards NPs that are in real concentrations (low concentrations, between 0.4 to 1.7%) in a material. All the mortars studied contained just few percentage of NPs, just enough to bring beneficial effects to the material. Whether in powder form (synthesis of NPs, manufacturing of the mortar) or in solid state (mortar with water, applying on a wall) or in sol-gel state (liquid mortar), we never observed SiO_2, TiO_2, nanoclay or nanocellulose inside PPEs. We only observed that the sol-gel state (liquid state) applying with an air gun can project particles in a bigger area. In this case, TiO_2 NPs were observed closed to the air gun on the gloves but not on masks and Tyvek where we detected all the other components of the mortar. This liquid state is very different from the other powder and solid states. The part focused on diffusion experiments was not based on real scenarios and were made at lab scale. Industrial partners sent us NPs and we made solutions. All these particles were at first observed and we saw that they were not single but were agglomerated and the size of these clusters were not in the nano range size (SEM, TEM, DLS, FFF). Concerning the aerosol diffusion, the concentration of solutions were chosen in function of the NPs size generated; the concentrations selected were in order to have a mean diameter of the aerosolized particles of about 100nm. According to the NPs investigated, the results were different although all the aerosolized particles were in the nano range size (FMPS measurements). Generally, SiO_2 and TiO_2 diffused less through clothes than nanoclay and nanocellulose. We observed too that the fleece jacket, that was thicker than the polyester 65%/cotton 35% material, was more efficient to the diffusion of all the NPs investigated. It seemed that the fleece jacket kept more NPs within due to its thickness its important porosity but although because this material is non-woven. The most efficient cloth for workers was the raining coat which was composed of two layers of polyamide and polyurethane because no NPs diffused through it. Concerning the liquid diffusion, we observed different results because the fleece jacket was the less efficient toward liquid diffusion of SiO_2 NPs compared to the polyester 65%/cotton 35% material. In this case, as the fleece jacket was a non-woven material, it can swell with liquid and enhances the diffusion of particles. For the both materials polyester 65%/cotton 35% and PA/PU, the diffusion experiments took more time, the kinetics were slower. We saw too that the rain coating was the most efficient because no NPs were observed in the downstream part of the diffusion cell. In the case of the liquid diffusion, we saw that particles were very big because we observed aggregates in the both parts of the cell which disturbed the ICPMS measurements and we thought that all the liquid samples taken during the kinetic were very inhomogeneous. We thought also that the problem of the kinetic in the upstream side for the polyester 65%/cotton 35% material and the PA/PU material were due to an anchoring of the NPs on the walls of the cell and/or on/in the material whereas its only due to the anchoring on the walls in the downstream side.

5. CONCLUSION

All the PPEs involved in real scenarios (gloves, masks, tyveks) showed that they were enough efficient in standard conditions. All the results are summarized in Tables 19 and 20. All the PPEs studied were efficient toward all the components contained in the solid and in the liquid states of the mortar during the entire life cycle of the NPs (Table 19). PU coated PA was the most efficient cloth towards aerosolized and hydrosol NPs. All the clothes were efficient toward aerosolized nanoSiO_2. The fleece jacket, that was thicker, hold nanoTiO_2 and not nanocellulose and nanoclay. Polyester 65% / cotton 35% seems to be the less efficient cloth (Table 20).

In perspective, it would be interesting to focus studies on a woven and a non-woven cloth with varying thickness for the both cases to investigate more precisely the role of the thickness and of the weaving. It would be also interesting to compare our lab-scale studies to real scenarios to study clothes wearied by a person in a room where aerosolized NPs will be generated.

Stages PPEs	Producing TiO_2	Manufacturing mortar (TiO_2, SiO_2, Mg)	Applying in a solid state (TiO_2, SiO_2, Mg)	Applying in a liquid state (spray) (TiO_2, SiO_2, Mg)	Demolishing a building (TiO_2, SiO_2)
gloves	efficient	efficient	efficient	efficient	n.a.
masks	n.a.	efficient	efficient	efficient	efficient
tyveks	efficient	n.a.	n.a.	efficient	n.a.

Table 19: Summary of results obtained on PPEs (gloves, masks, Tyvek) used in 5 real scenarios.

	SiO_2 aerosol	SiO_2 hydrosol	TiO_2 aerosol	Nanocellulose aerosol	Nanoclay aerosol
100% polyester (fleece jacket)	efficient	Not efficient	efficient	Not efficient	Not efficient
Polyester 65%/ cotton 35%	efficient	Not efficient	Not efficient	Not efficient	Not efficient
PU coated PA rain cloth	efficient	efficient	efficient	efficient	efficient

6. LIST OF FIGURES

7. LIST OF TABLES

8. APPENDIX

Images of SEM observation of all the PPEs involved in real scenarios:

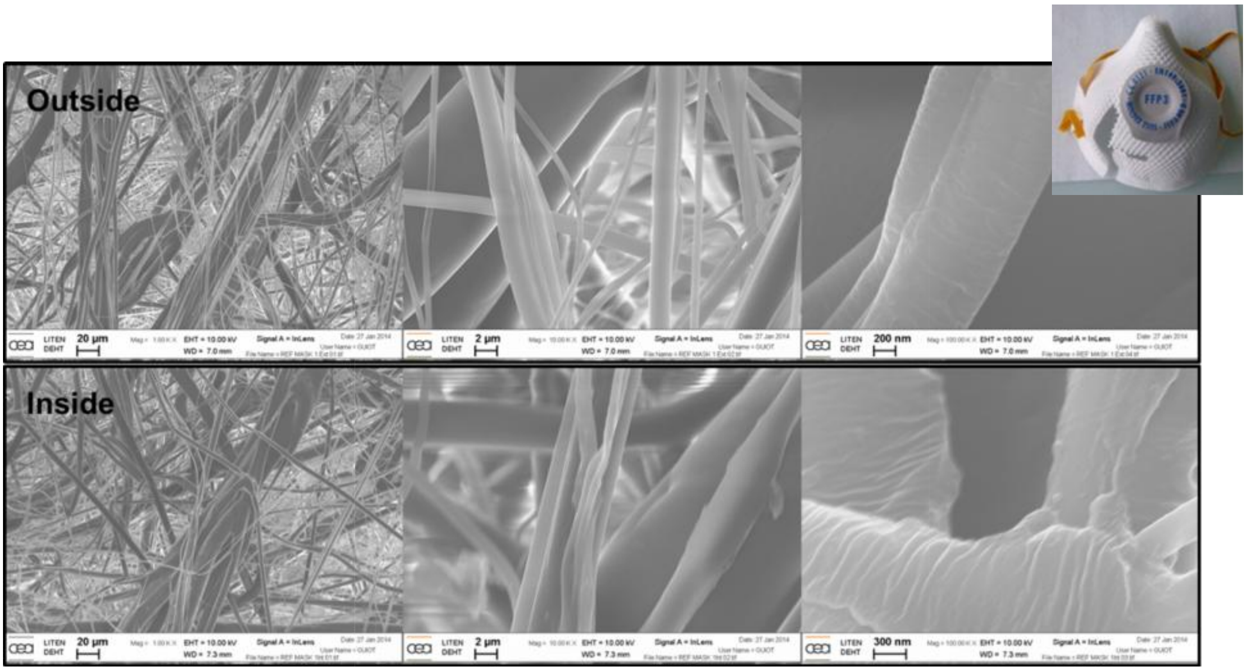

Figure 25: SEM characterization of Ref-MASK-1.

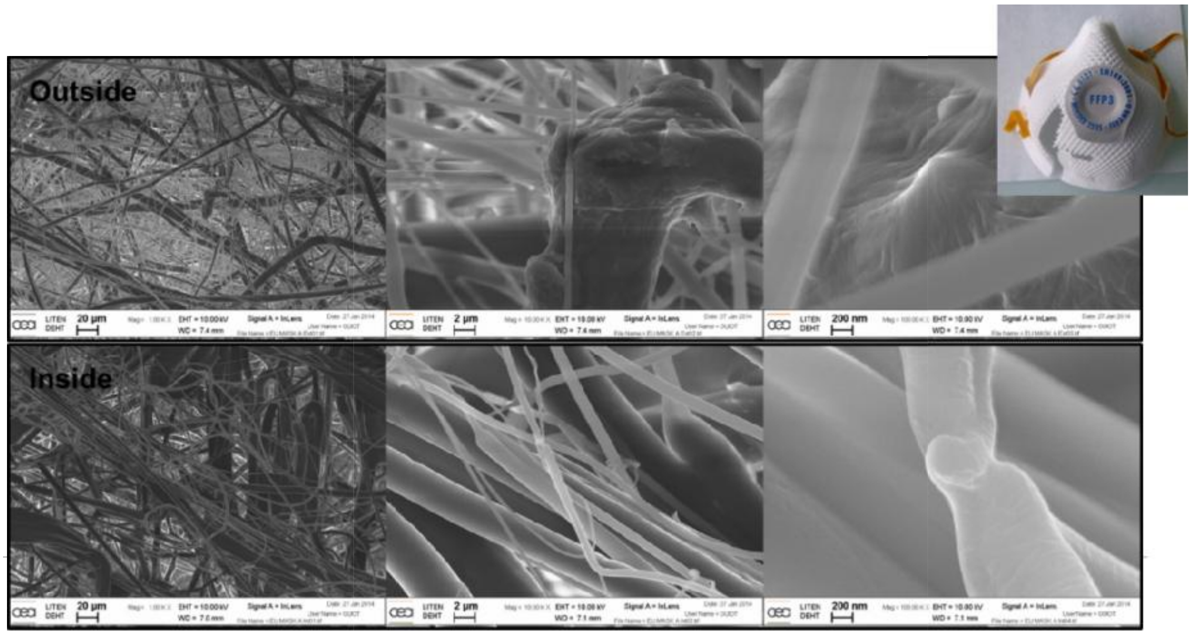

Figure 26: SEM characterization of EU-MASK-A.

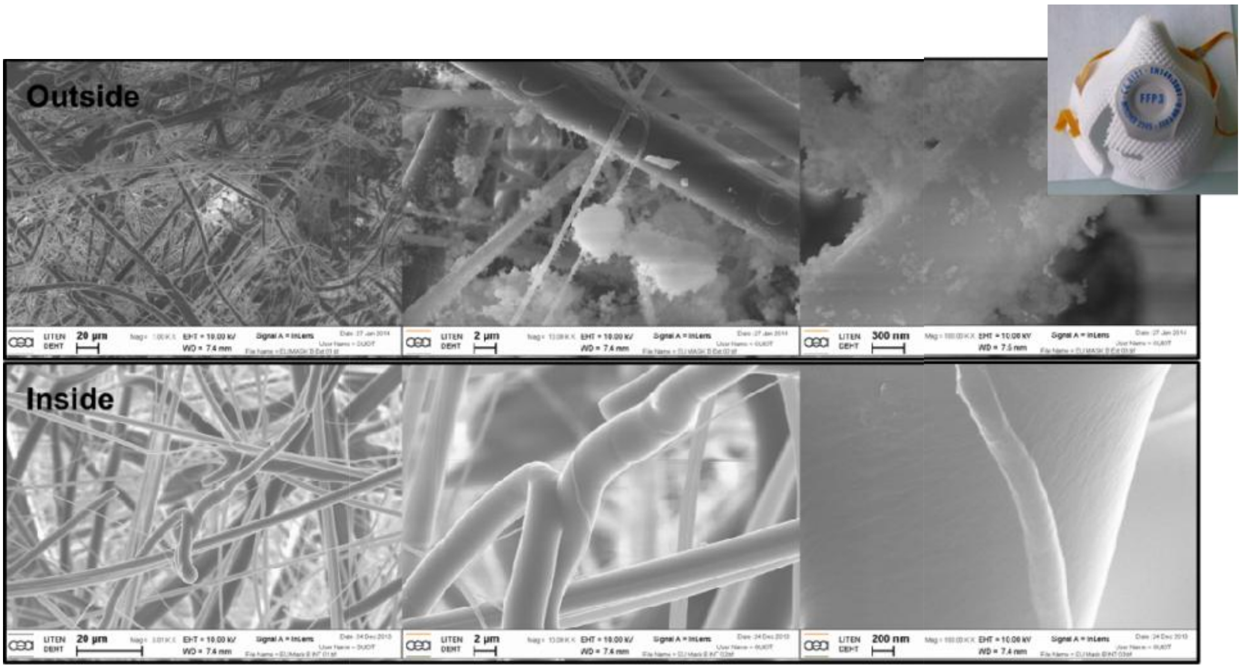

Figure 27: SEM characterization of EU-MASK-B.

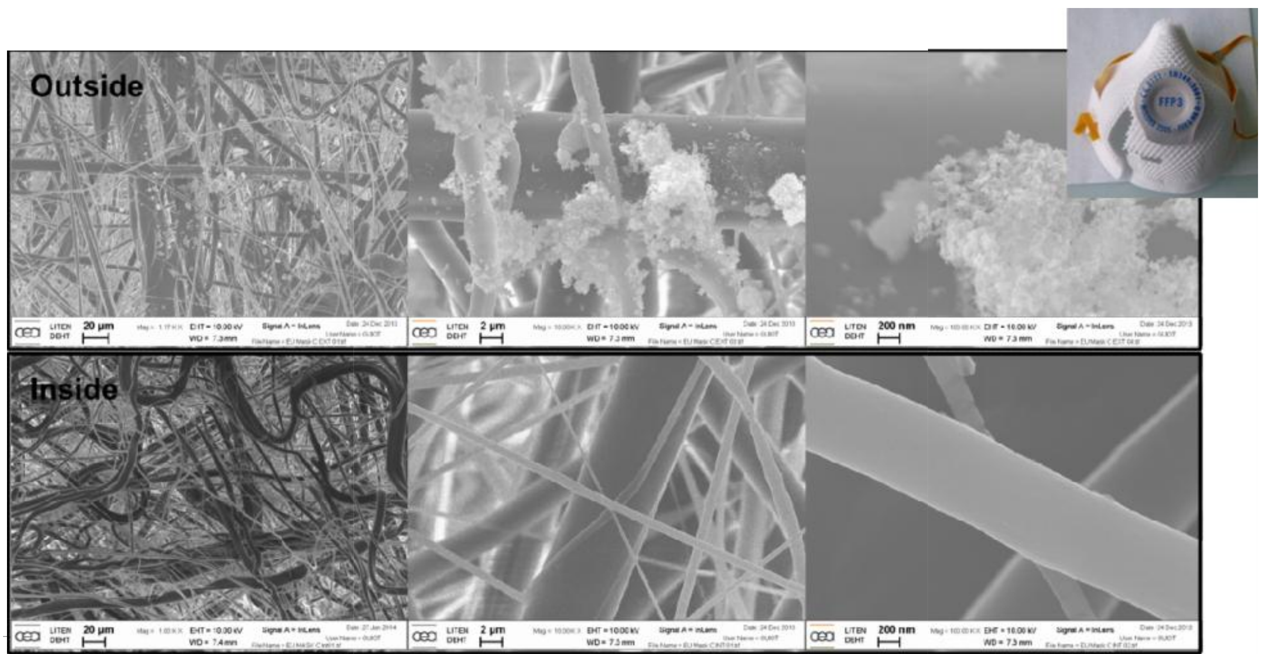

Figure 28: SEM characterization of EU-MASK-C.

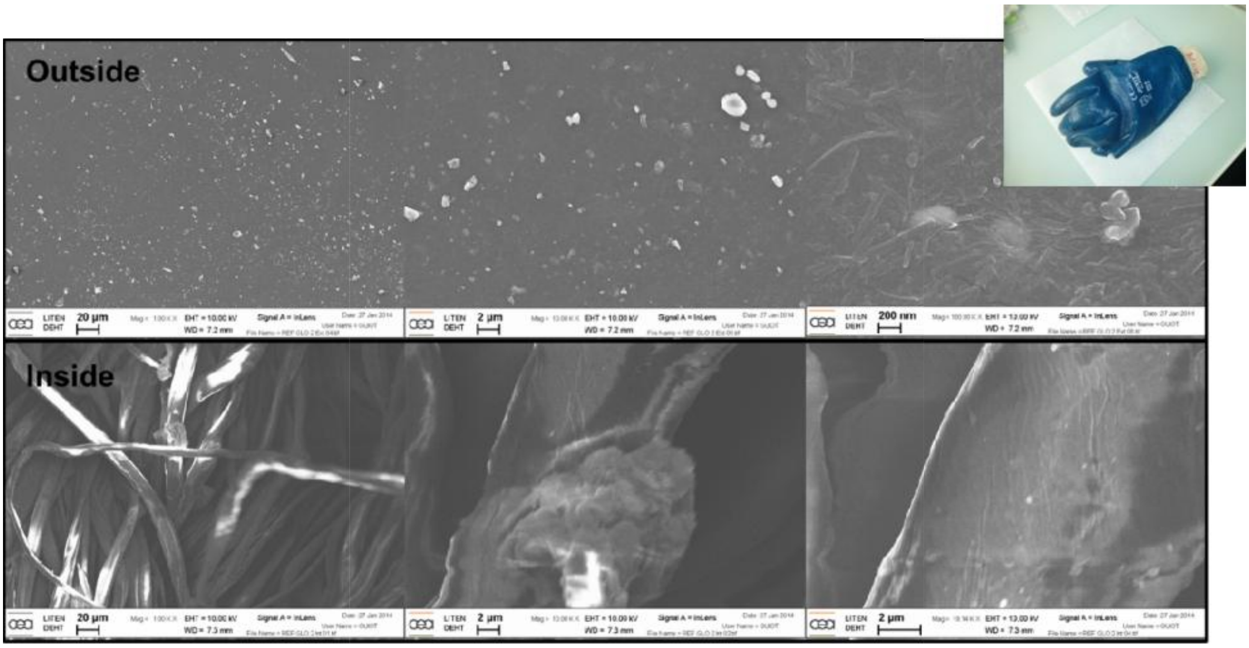

Figure 29: SEM characterization of Ref-GLO-2.

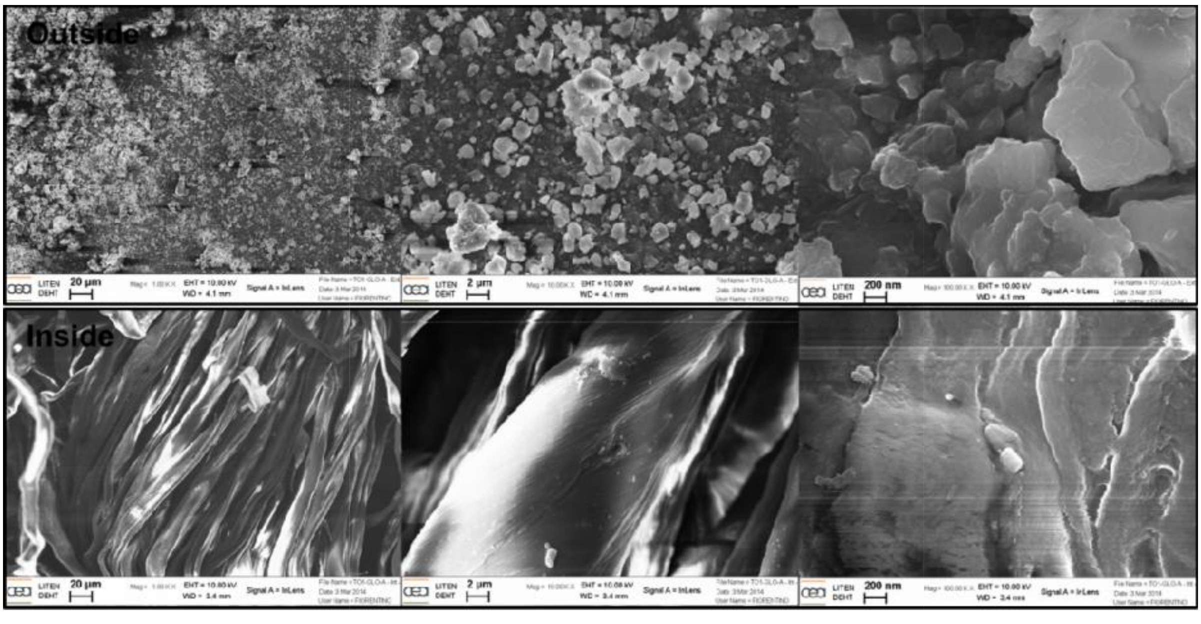

Figure 30: SEM characterization of T01-GLO-A.

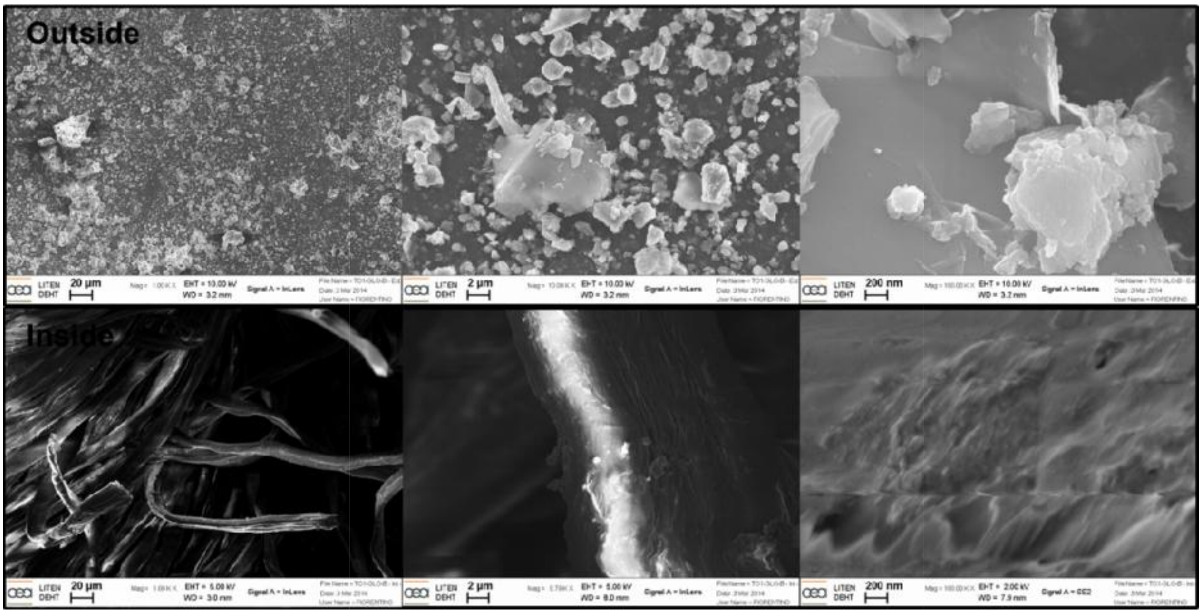

Figure 31: SEM characterization of T01-GLO-B.

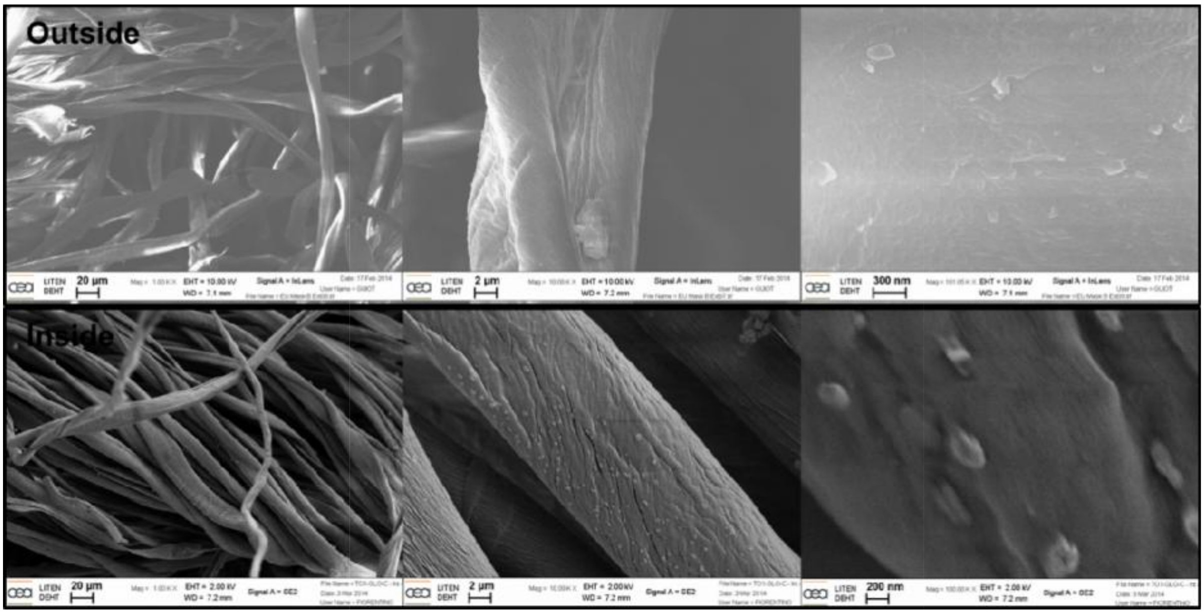

Figure 32: SEM characterization of T01-GLO-C.

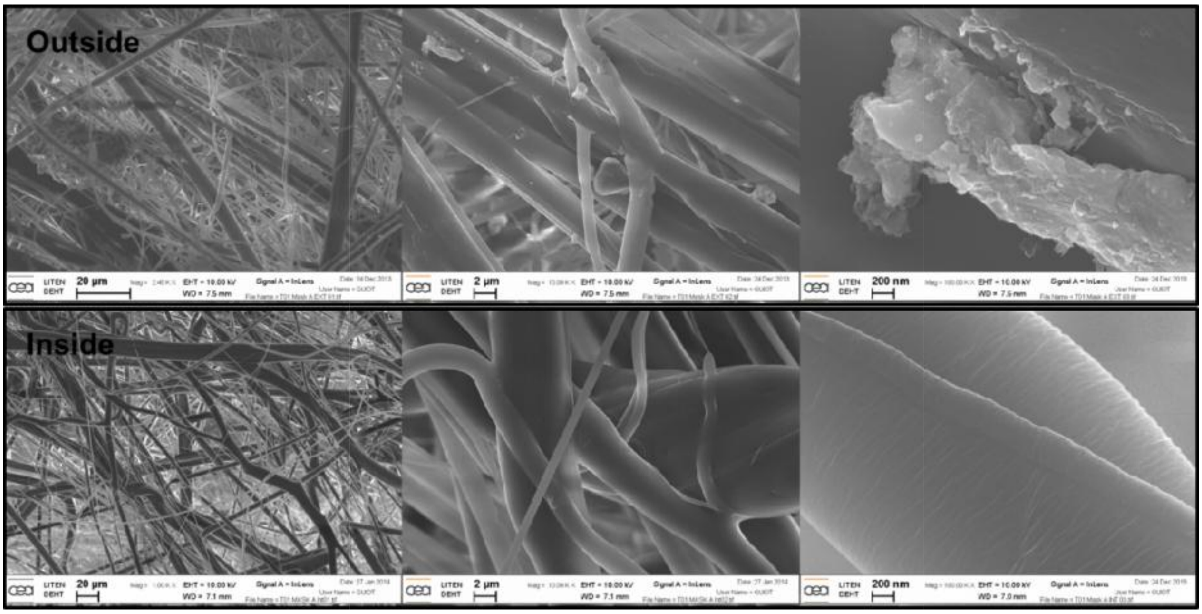

Figure 33: SEM characterization of T01-MASK-A.

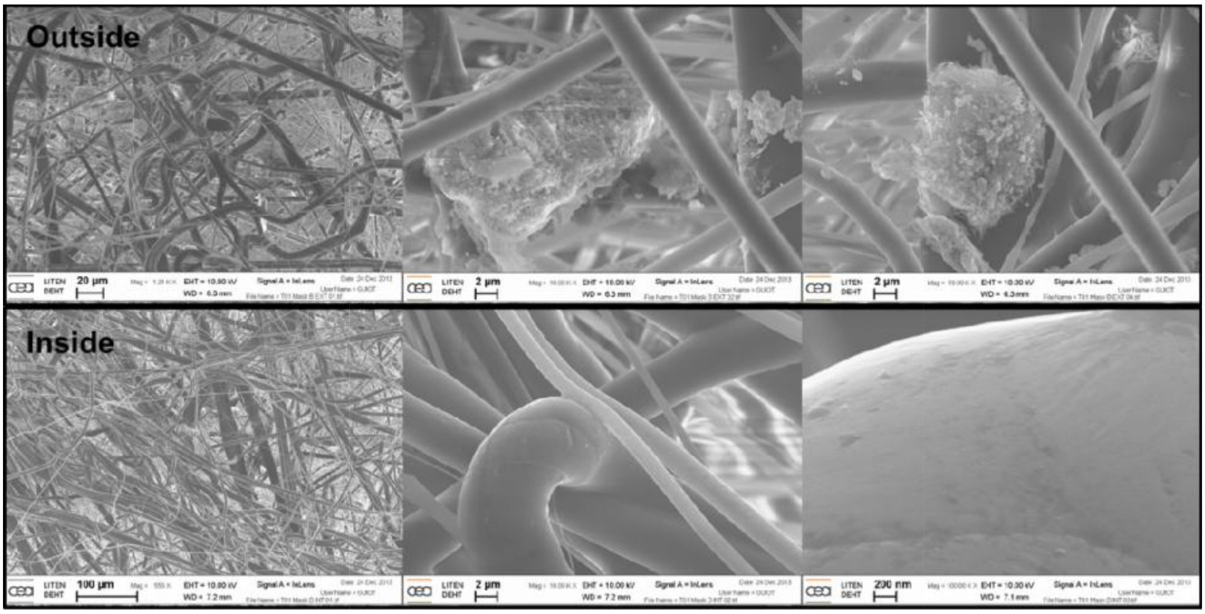

Figure 34: SEM characterization of T01-MASK-B.

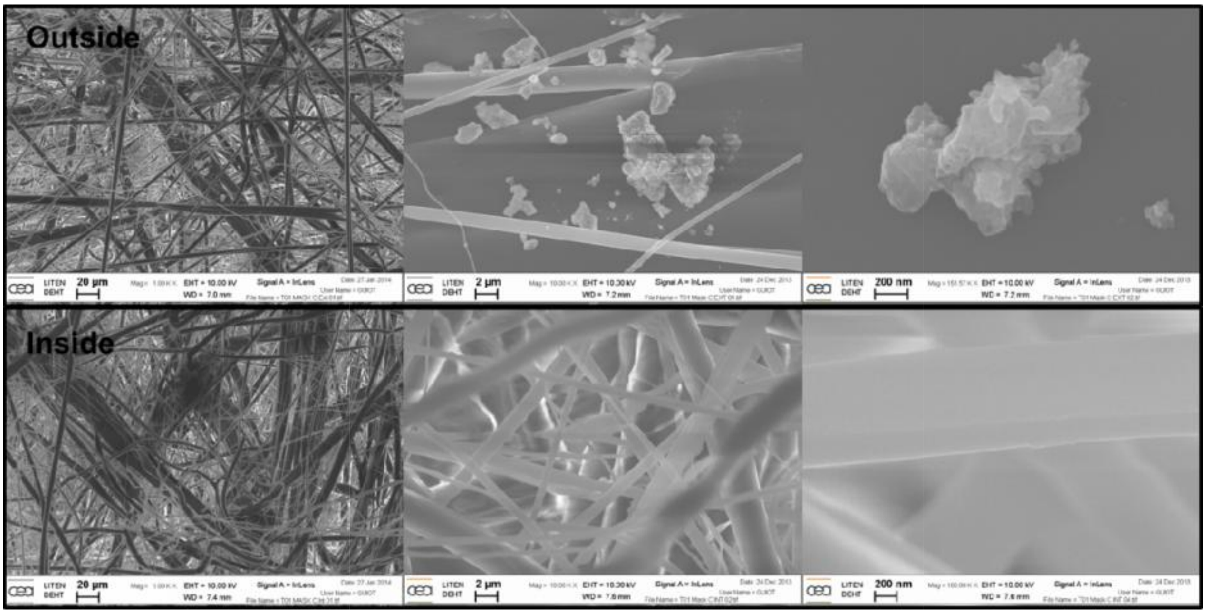

Figure 35: SEM characterization of T01-MASK-C.

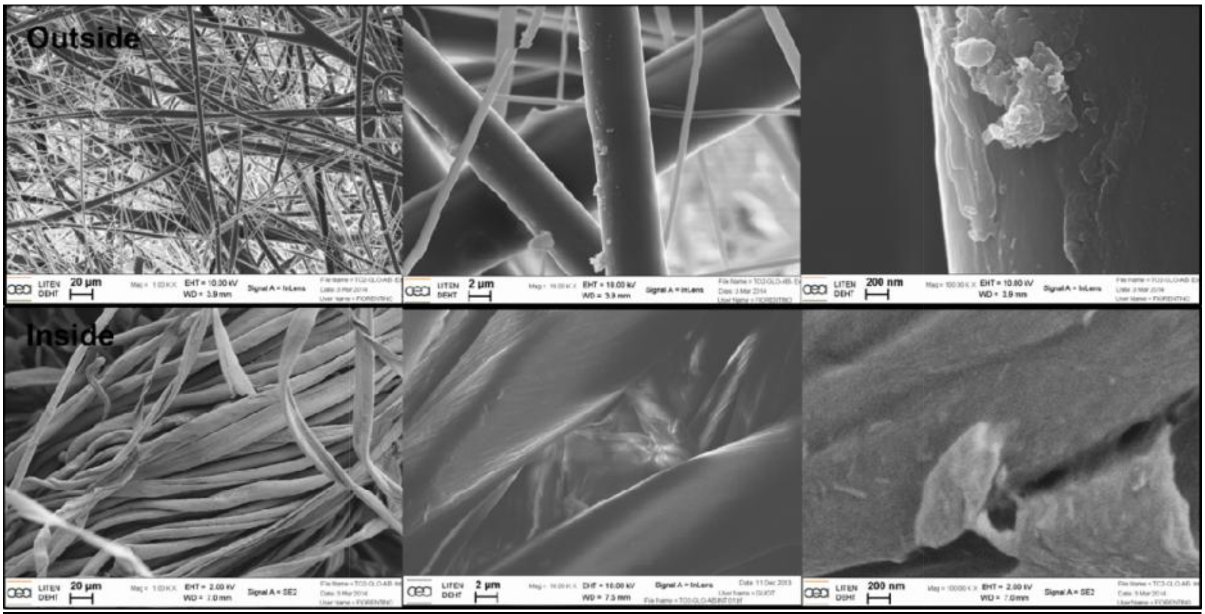

Figure 36: SEM characterization of T02-GLO-AB.

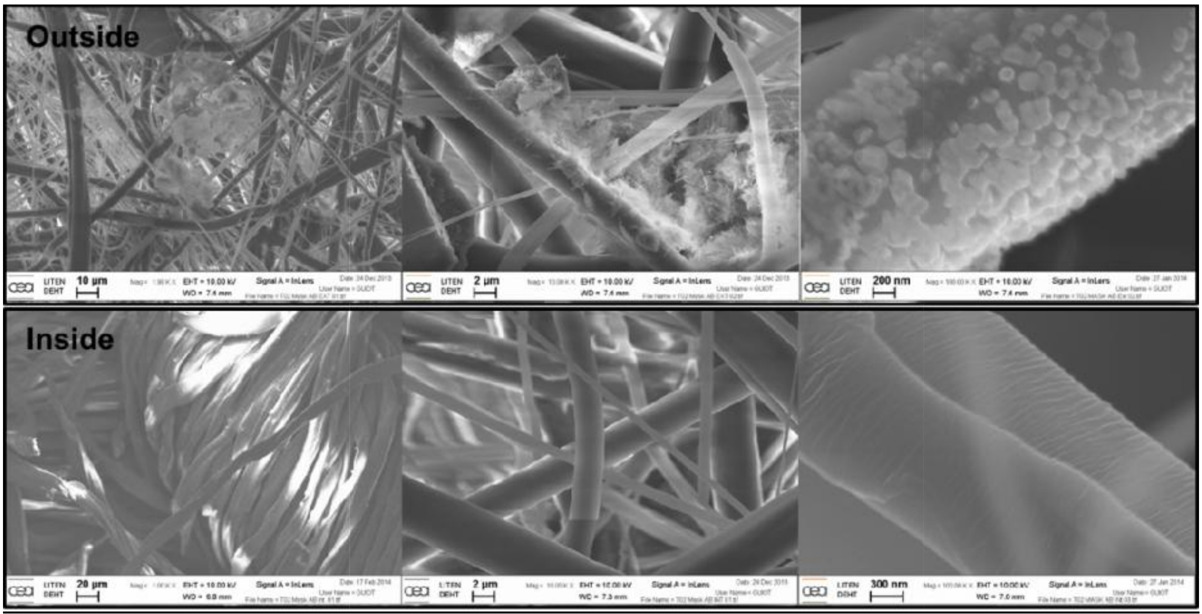

Figure 37: SEM characterization of T02-MASK-AB.

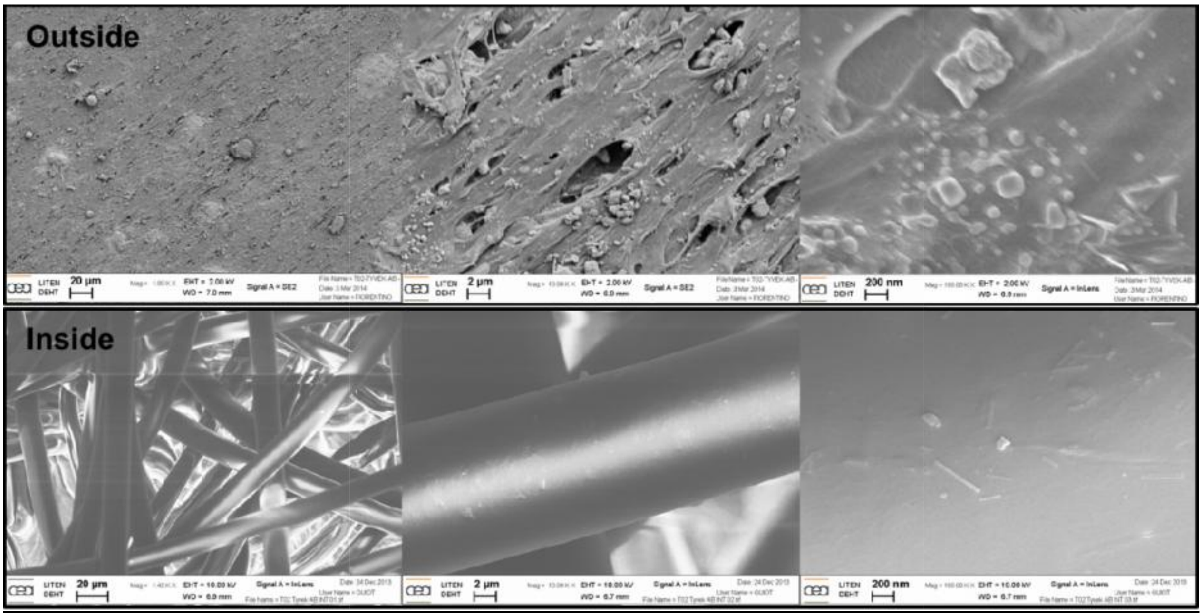

Figure 38: SEM characterization of T02-TYVEK-AB.

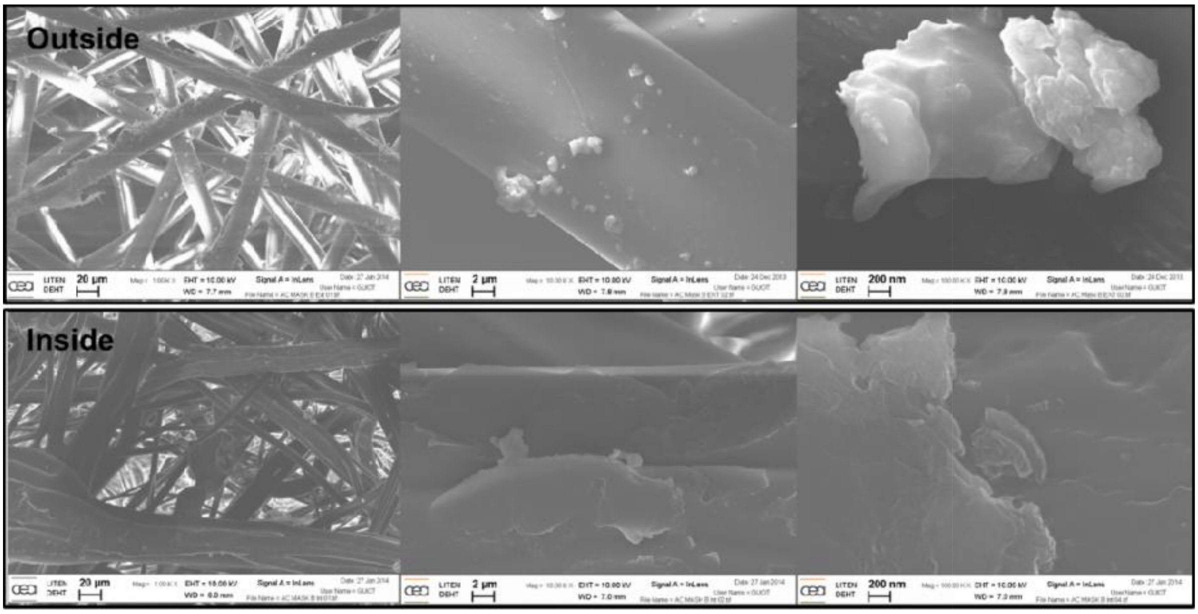

Figure 39: SEM-EDX characterization of AC-MASK-B.

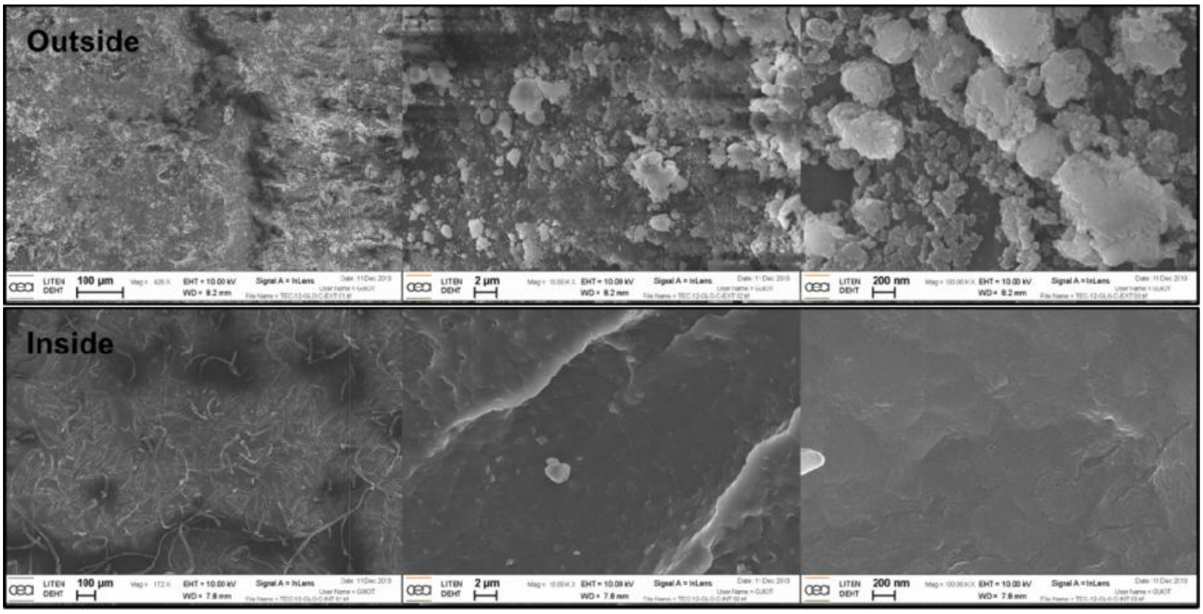

Figure 40: SEM characterization of TEC12-GLO.

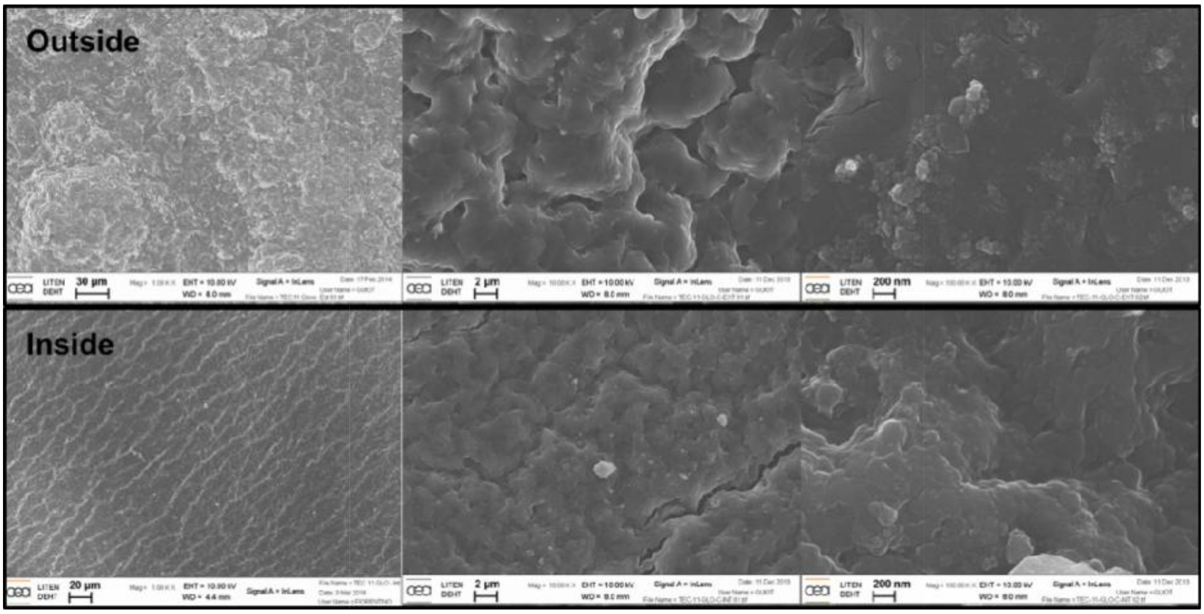

Figure 41: SEM characterization of TEC11-GLO.

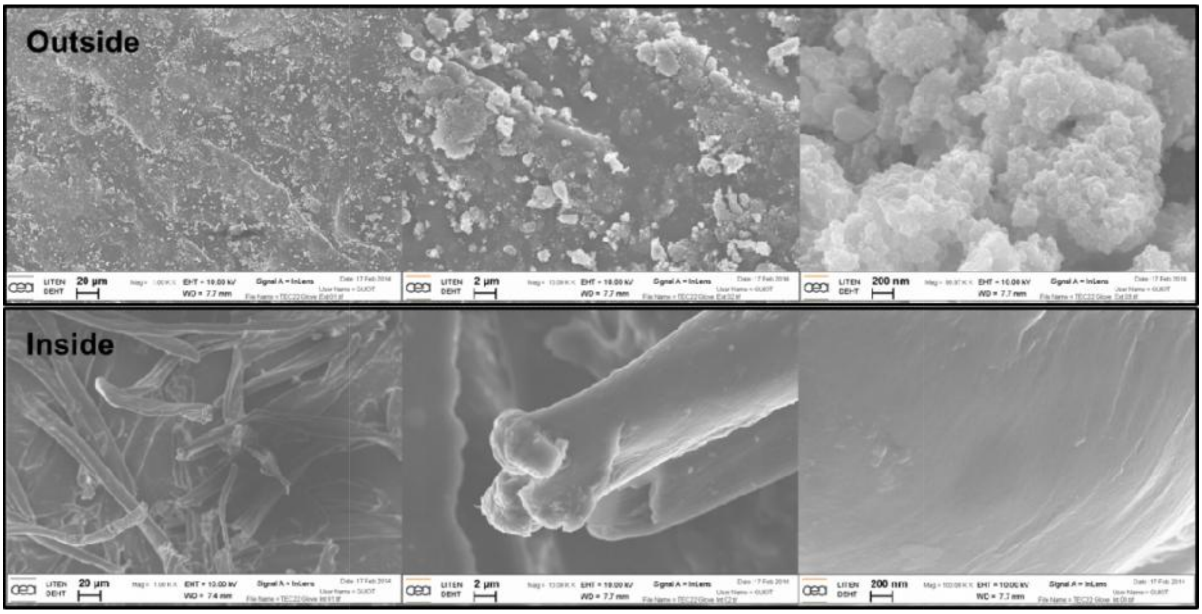

Figure 42: SEM characterization of TEC22-GLO

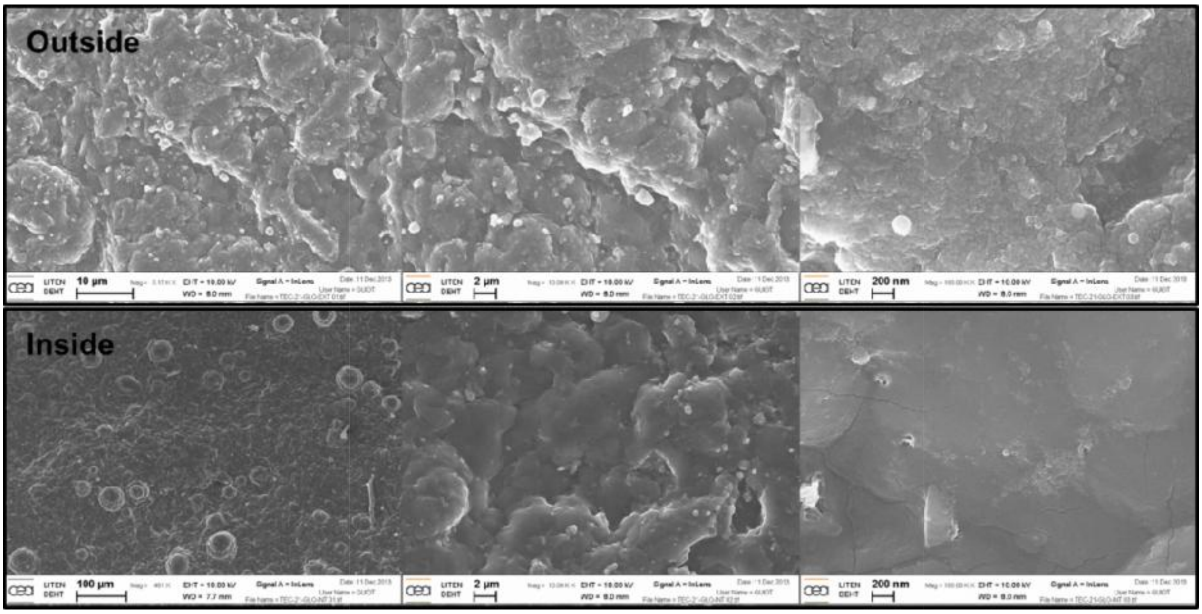

Figure 43: SEM-EDX characterization of TEC21-GLO.

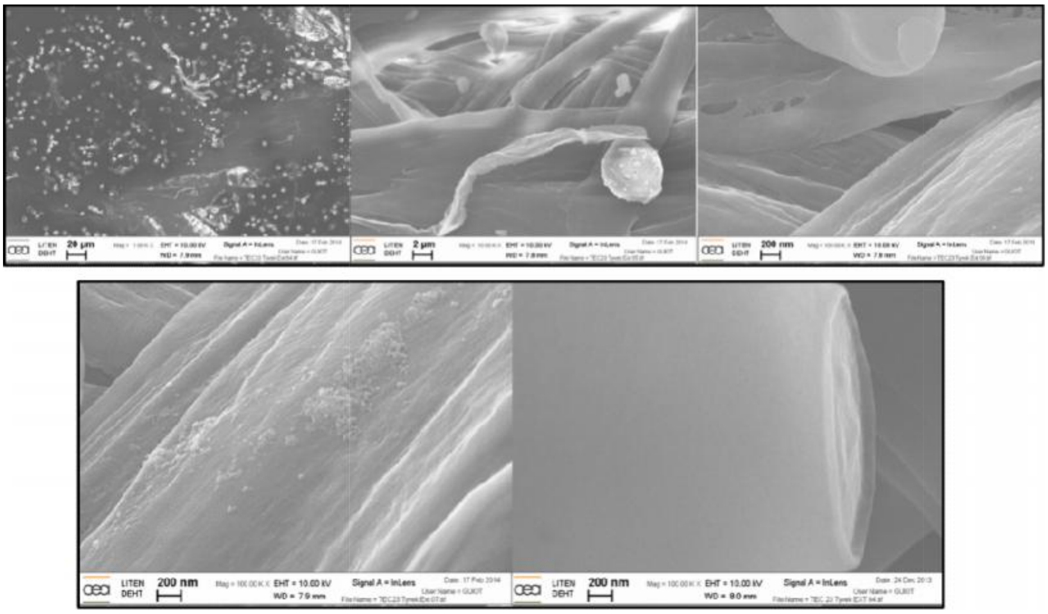

Figure 44: SEM characterization of TEC23-TYVEK outside.

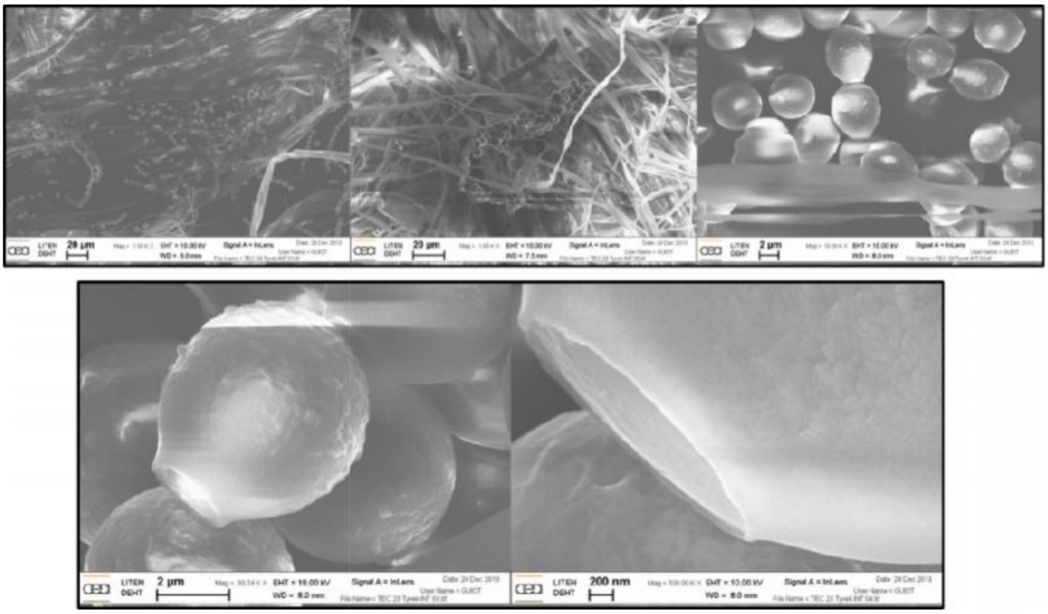

Figure 45: SEM characterization of TEC23-TYVEK inside.